Russian Chemical Reviews **70** (2) 131 – 146 (2001) © 2001 Russian Academy of Sciences and Turpion Ltd

DOI 10.1070/RC2001v070n02000621

Hydrogen-containing carbon nanostructures: synthesis and properties

B P Tarasov, N F Goldshleger, A P Moravsky

Contents

I. Introduction 131
II. Synthesis of hydrofullerenes 131
III. Properties of hydrofullerenes 135
IV. Sorption of hydrogen by carbon nanotubes and graphite nanofibres 138
V. Conclusion 143

Abstract. Data on the interaction of carbon nanomaterials (fullerenes, carbon nanotubes, graphite nanofibres and their metal-doped modifications) with hydrogen are surveyed. New results on the preparation and properties of hydrofullerenes are presented. The prospects for the use of carbon nanomaterials as reversible hydrogen sorbents are discussed. The bibliography includes 183 references.

I. Introduction

Hydrogen has indisputable advantages over other energy carriers as it is a versatile, highly efficient and environmentally safe energy carrier. This provides good prospects for its wide application in power engineering, especially as a fuel for vehicles transport.[1] However, there is a very serious problem hampering the use of hydrogen as a fuel, namely, hydrogen storage and transportation. None of the currently available methods for the storage of hydrogen (in the gas state under high pressure, in the liquid state, as metal hydrides and hydrides of intermetallic compounds, or in the adsorbed state at low temperatures, see Table 1) meets the requirements imposed on hydrogen storage systems, *e.g.*, by the US Department of Energy (DOE) Hydrogen Plan (content of hydrogen $\geqslant 6.5$ mass % or $\geqslant 63$ kg m^{-3})[2] and by the International Energy Agency (content of hydrogen $\geqslant 5$ mass %, release of hydrogen at temperatures below 373 K).[3] Therefore, the development of new, more efficient methods for the storage and transportation of hydrogen is still an important task the success of which will determine, in many respects, further progress in the development of the 'hydrogen' technology and power engineering.

Hydrogen accumulation based on the reversible sorption of hydrogen is one of the most promising and popular methods for the storage of hydrogen. The most popular sorbents include hydride-forming metals and intermetallic compounds[4,5] as well as active carbons prepared by various methods.[6–9] Fullerenes and their derivatives, carbon nanofibres and nanotubes have been suggested repeatedly over recent years as hydrogen-accumulating substrates.[2,6,10,11] In the present review, we consider the data on the interaction of molecular hydrogen with these carbon nanomaterials (NM) and the prospects for their application as reversible sorbents for the storage of hydrogen.

Table 1. Traditional hydrogen storage methods.[3]

Method and conditions for hydrogen storage	Hydrogen content in the sorbent (mass %)	Hydrogen volume content /kg m^{-3}	Drawbacks of the method
Gaseous H_2 (300 K, 10 MPa)	100	7.7	heavy containers, small volume capacity
Liquid H_2 (20 K)	100	71	high losses, high cost
Metal-hydride			
TiH_2	4.0	150	insufficient
MgH_2	7.6	120	capacity; necessity
$LaNi_5H_{6.7}$	1.4	85	of heating;
$TiFeH_2$	1.9	95	sensitivity
Mg_2NiH_4	3.7	80	to admixtures
Cryoadsorption activated carbon (155 K, 6.9 MPa)	0.05 – 2	~1 – 2	necessity of cooling and compression

II. Synthesis of hydrofullerenes

The presently known methods for the preparation of hydrofullerenes,† such as the Birch – Hückel reduction of fullerenes, hydroboration, catalytic hydrogenation of fullerenes, reduction of fullerenes based on non-catalytic transfer of hydrogen from a donor to an acceptor, *etc.*, have been surveyed in detail in several reviews.[12–14] However, the rapid development of studies in this field requires a continuous analysis of the newly appearing methods for the synthesis of hydrofullerenes, especially because no ideal procedure for the preparation of hydrofullerenes with reliably controlled composition is yet available.

B P Tarasov, N F Goldshleger, A P Moravsky Institute of Problems of Chemical Physics, Russian Academy of Sciences, 142432 Chernogolovka, Moscow Region, Russian Federation. Fax (7-096) 576 40 09. Tel. (7-095) 913 21 09. E-mail: btarasov@icp.ac.ru (B P Tarasov), gold@cat.icp.ac.ru (N F Goldshleger), moralex@icp.ac.ru (A P Moravsky)

Received 18 August 2000
Uspekhi Khimii **70** (2) 149 – 166 (2001); translated by S S Veselyi

† Hydrofullerenes are also called fullerene hydrides or hydrogen-containing fullerene compounds; sometimes they are also called hydrofullerites in order to emphasise the solid state of the product.

1. Hydrogenation of fullerites and metal fullerides with molecular hydrogen

Chemical transformations occurring in mechanical mixtures of powders of a fullerite (C_{60}, C_{60}/C_{70}) and hydrogen-sorbing metals and intermetallic compounds (Pd, V, $LaNi_5$, $LaNi_{4.65}Mn_{0.35}$, $CeCo_3$) under the action of molecular hydrogen or deuterium have been studied in a wide pressure and temperature range.[15–19] It has been found that hydrogenation at 1.0–5.0 MPa and 573–673 K results in mixtures of metal hydrides MH_y and hydrofullerenes $C_{60}H_x$:

$$\{C_{60} + M\} + H_2 \longrightarrow \{C_{60}H_x + MH_y\}.$$

Heating of the resulting mixture $\{C_{60}H_x + MH_y\}$ in an inert atmosphere results first in dehydrogenation of the metal hydride and then (at 800 K) dehydrogenation of the hydrofullerene to give hydrogen and fullerene–metal compositions.‡

$$\{C_{60}H_x + MH_y\} \xrightarrow[-H_2]{<600\ K} \{C_{60}H_x + M\} \xrightarrow[-H_2]{\sim 800\ K} \{C_{60} + M\}.$$

Hence, we are dealing with a system which can accumulate hydrogen under certain conditions and release it under other conditions. This reaction cycle can be repeated many times, but the side reactions, such as polymerisation and carbide formation, restrict the prospects of application of these systems for hydrogen accumulation.

Depending on the temperature, the reaction of the pre-synthesised fullerides $C_{60}Pt$ and $C_{60}Pd_{4.9}$ with hydrogen (the H_2 pressure being 1–3 MPa) results either in hydrogen compounds of metallofullerides $<C_{60}MH_x>$ or in mixtures of hydrofullerenes $C_{60}H_x$ ($x = 2–26$) with Pt or PdH_y, respectively.

$$C_{60}Pt + H_2 \xrightarrow{400–550\ K} <C_{60}PtH_x>$$
$$C_{60}Pt + H_2 \xrightarrow{600–700\ K} C_{60}H_x + Pt$$

$$C_{60}Pd_{4.9} + H_2 \xrightarrow{400–550\ K} <C_{60}Pd_{4.9}H_x>$$
$$C_{60}Pd_{4.9} + H_2 \xrightarrow{600–700\ K} C_{60}H_x + PdH_y$$

Upon heating to 800 K, almost all the hydrogen is evolved from the reaction products, and the resulting mixture of the fullerite with the metal (Pd, Pt) can be hydrogenated again in the temperature range from 400 to 700 K to give mixtures of the hydrofullerene with PdH_y or Pt.[20–22]

The source of gaseous hydrogen and its purity affect considerably the hydrogenation of solid fullerenes and the state of the reaction products. For example, the hydrogenation of crystalline fullerene (fullerite) with hydrogen evolved upon the decomposition of hydrides of intermetallic compounds results in crystalline hydrofullerenes containing from 10 to 30 hydrogen atoms per fullerene molecule.[23,24] The content of hydrogen in the product increases with the number of the 'heating to 673 K–cooling to 300 K' cycles. The thermal cyclic hydrogenation mode not only provides a deeper process but also gives samples with a more homogeneous distribution of the components over the volume. The IR spectra of the resulting hydro- or deuteriofullerenes show intense absorption bands in the regions of C–H (2800–3000 cm^{-1}) and C–D (2050–2200 cm^{-1}) stretching vibrations. The relative intensities of the absorption bands of the starting C_{60} decrease abruptly (Fig. 1).

X-Ray diffraction analysis of the reduction product shows that hydrofullerene $C_{60}H_x$ (or deuteriofullerene $C_{60}D_x$) retains the crystal structure of the parent fullerite; the a_0 parameter of the face-centred cubic (FCC) lattice increases monotonically with the amount of hydrogen (or deuterium) in the hydrofullerene (Fig. 2).§

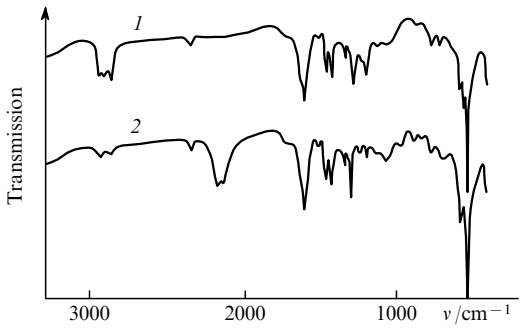


Figure 1. IR spectra of hydro- (*1*) and deuteriofullerenes (*2*) $C_{60}H(D)_{18–24}$.[24]

Heating of the hydrides synthesised by this method to 800 K results in intense evolution of hydrogen. The IR spectrum of the solid product of the thermal decomposition of hydrofullerene manifests bands corresponding to C_{60} and a series of bands the positions of which are close to those of the photo- or thermobarically polymerised C_{60} with the cyclobutane rings between the fullerene molecules,[26] which indicates that thermal dehydrogenation is accompanied by polymerisation of the fullerene cages.

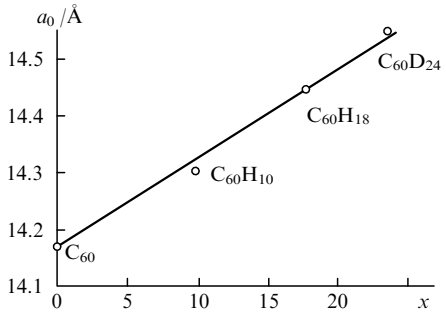


Figure 2. Dependence of the FCC lattice parameter a_0 of hydro- and deuteriofullerenes $C_{60}H(D)_x$ on the number of hydrogen and deuterium atoms.[25]

The samples dehydrogenated at 800 K can be hydrogenated again, but repeated 'hydrogenation–dehydrogenation' cycles result in the accumulation of polymerised fullerene.[25] The addition of NH_3, HI or C_2H_5I (5 mass %–10 mass %) to the hydrogen evolved from a metal-hydride accumulator accelerates considerably the hydrogenation of the fullerite but also increases the degree of polymerisation of the fullerene molecules formed upon the dehydrogenation of the hydrofullerene.[3]

Studies of the magnetic properties of hydrofullerenes prepared by hydrogenation of fullerene with hydrogen liberated from an accumulator based on hydrides of intermetallic compounds of nickel and rare-earth metals [23] showed that the samples contained ferromagnetic particles; this was explained by the gas-phase transfer into the reactor of traces of metal or metal hydride particles by hydrogen which has evolved from the accumulator. One could assume that fine particles of nickel and/or nickel–rare-earth metal intermetallides act as catalysts of the solid-phase hydrogenation of fullerene. The use of a nickel catalyst for hydrogenation of solid fullerite, *e.g.*, by controlled addition of volatile nickel compounds to the gas fed into the reactor, could

‡ In certain cases, heating above 950 K results in irreversible formation of metal carbides.

§ According to the reported data,[25] the lattice parameters for $C_{60}H_x$ and $C_{60}D_x$ are similar for equal x values.

provide more efficient reversible systems for hydrogen accumulation.

The solid-phase hydrogenation of fullerenes continues to attract the attention of scientists from the viewpoint of both practical application (hydrogen storage) and synthesis of individual hydrofullerenes. For example, solid-phase deuteration of C_{60} at 373–773 K and p_{D_2} = 15 MPa gave deuterides with the compositions $C_{60}D_8$, $C_{60}D_{18}$ and $C_{60}D_{36}$ (FCC structure, a_0 = 1.423, 1.448 and 1.500 nm, respectively).[27] Controlled doping of fullerene with palladium decreases (down to 373 K) the temperature of hydrogen or deuterium sorption relative to that for the undoped C_{60} sample at a gas (H_2 or D_2) pressure of 100 MPa.[28] A neutron diffraction study of palladium-doped fullerene showed no characteristic peaks of metallic Pd. Similarly, these peaks were not observed in the samples treated with hydrogen. Treatment of fullerene-containing carbon black by hydrogen plasma gives hydrofullerenes with low hydrogen content (x = 1–6).[29] Prolonged treatment does not increase the amount of sorbed hydrogen.

Progress is also observed in the field of liquid-phase hydrogenation of fullerenes. Cheaper heterogeneous catalysts have been developed and methods for more selective and extensive hydrogenation have been found. For example, the hydrogenation of C_{60} on the Ni/Al_2O_3 catalyst[30] occurs under milder conditions (toluene, 423–523 K, 2.5–7.5 MPa) than the hydrogenation on the Ru/C catalyst.[31] The reaction occurs selectively to give $C_{60}H_{36}$. The reaction selectivity can primarily be accounted for by the high dispersion of nickel deposited onto Al_2O_3.¶ A decrease in the reaction temperature decreases the selectivity (similarly to the reduction of C_{60} with dihydroanthracene in the presence of an organic catalyst[32]).

Liquid-phase hydrogenation of C_{60} with hydrogen (at atmospheric pressure, in the presence of 4% Pd/SiO_2, 5% Ru/Al_2O_3 or 5% Rh/Al_2O_3) or with hydrogen donors (cyclohexane, decalin, *etc.*) at 323–343 and 348–433 K, respectively, results in hydrofullerenes $C_{60}H_x$.[33] In some experiments, Pd/SiO_2 was used as the catalyst for the hydrogenation of fullerene by hydrogen transfer from a donor (cyclohexane, cyclohexene) to the acceptor (C_{60}). Titration of the hydrogen peroxide formed due to the oxidation of $C_{60}H_x$ with 2-ethylanthraquinone in the presence of O_2, chemical determination of hydrogen in $C_{60}H_x$, as well as IR and NMR spectra indicate that the C_{60} reduction products have the composition $C_{60}H_{42-46}$.[33] Unfortunately, the results of mass spectrometric determination of the hydrofullerenes formed have not been reported; this might provide direct information on the composition of $C_{60}H_x$.[33]

In a search for systems for the hydrogenation of fullerenes and dehydrogenation of hydrofullerenes which would comply with the requirements for the practically applicable hydrogen accumulators, Loutfy *et al.*[34] have examined whether soluble catalysts could be employed for hydrogenation of the C=C bonds and if salt melts could be used as the reaction media for hydrogenation. They also studied the effect of modification of the fullerene electronic structure on the hydrogenation process. This approach was based on the achievements in studies of the activation of the C–H bonds by metal complexes,[35] on the one hand, and on the data on the efficient catalytic hydrogenation of the C=C bonds with hydrogen in the presence of Cs_6C_{70},[36] on the other hand. Alkoxy compounds of the Group IV metals were found to be efficient as the soluble catalysts for fullerite hydrogenation and hydrofullerite dehydrogenation. This study[34] has shown that the use of certain soluble catalysts made it possible to decrease considerably the activation energy of hydrogenation and the temperature of the process. For example, the dehydrogenation of $(C_{60}/C_{70})H_{36}$ occurred at 573 K (6 h) to give $(C_{60}/C_{70})H_{22}$ (the loss of 1.74 mass % H_2), while the repeated hydrogenation of $(C_{60}/C_{70})H_{22}$ occurred at 423 K (12 h, 3.6 MPa) to give $(C_{60}/C_{70})H_{\sim 45}$. It has also been shown that doping of fullerene by an alkali metal facilitated markedly the fullerene hydrogenation. The dehydrogenation in this system occurs at considerably lower temperatures than the non-catalytic dehydrogenation of solid hydrofullerites.

The use of operating temperatures below 400 K is important for hydrogen-accumulating systems, hence these results[34] demonstrate that an almost acceptable temperature range can be achieved.

2. Reduction of fullerenes in the 'metal–hydrogen donor' system

The reduction of fullerenes is carried out using many traditional methods of organometallic chemistry (see, *e.g.*, the review[37]). For example, lithium in liquid ammonia in the presence of Bu^tOH was used for the reduction of C_{60}.[38]

$$C_{60} \xrightarrow{Li,\ NH_3\,(liq),\ Bu^tOH} C_{60}H_{2n}\,.$$

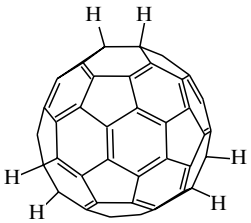
The process stopped in the step of the formation of $C_{60}H_{32-36}$ (see Refs 12 and 13). The products with a lower hydrogen content, *e.g.*, $C_{60}H_{32}$, were probably formed during the analysis or storage of the samples. The composition $C_{60}H_{36}$ of the reduction product of C_{60} fullerene with lithium in liquid ammonia has also been confirmed by other researchers.[39]

Polyfullerenes obtained by photo-induced and radical polymerisation of C_{60} cages (the radical polymerisation is preferable for the synthesis of polyfullerenes) are also reduced according to the Birch–Hückel method to give hydropolyfullerenes with a mean hydrogen content of ~3.5 mass % (for $C_{60}H_{36}$, 4.76 mass % H_2).[40] Hydropolyfullerenes, unlike monomeric hydrofullerenes with an equal hydrogen content, are almost insoluble in CS_2. This implies that the reduction at low temperatures does not involve cleavage of the C–C bonds between the fullerene cages in the polymers; this has been confirmed by gel-permeation chromatography. The IR spectra of hydropolyfullerenes contain intense bands in the region of C–H stretching vibrations. The ^1H and ^{13}C NMR spectra indicate structural similarity between polymeric and monomeric hydrofullerenes (the positions of the hydrogen atoms in the fullerene cage). The use of polyfullerenes does not increase the degree of hydrogenation of the fullerene cage, and hence, the amount of stored hydrogen. Thus, polyfullerenes are not superior to C_{60} molecules in hydrogenation and dehydrogenation reactions.

The reaction of C_{60} with $EtAlCl_2$ and activated magnesium [C_{60} : Al : Mg = 1 : (50–150) : (30–50); 293–295 K] in a THF–toluene mixture in the presence of Cp_2TiCl_2 (1 mol.%–3 mol.%) results in fullerene-containing aluminacyclopropane (yield 75%–90%), hydrolysis of which in D_2O results in a partially deuterated fullerene derivative.[41] Metallation of C_{60} with an excess of Et_3Al in the presence of Cp_2ZrCl_2 gives 2,3-fullerenoaluminacyclopentanes, hydrolysis of which results in mixtures of hydrogen-containing ethylfullerenes of the type $H_mC_{60}Et_m$ (m = 1–12).[42]

The reduction of C_{60} and C_{70} in the 'metal (M)–proton donor' system, where M = Zn (E° = −0.76 V), Ti (E° = −1.63 V), Al (E° = −1.66 V) or Mg (E° = −2.37 V), was also studied.[43–46] It was shown that the reaction of C_{60} with the Zn/Cu redox couple and a proton donor in toluene , unlike the reaction of C_{60} with Zn dust,[43] results in a more efficient fullerene reduction which occurs *via* the consecutive formation of $C_{60}H_2$, $C_{60}H_4$, and finally, $C_{60}H_6$; the target compounds can be isolated in each step.[44–47] Prolonged heating of a C_{60}–Zn/Cu–H_2O mixture in toluene results in two $C_{60}H_6$ isomers in the ratio 6 : 1, these amount to 30%–40% with respect to the starting C_{60}. The ^1H and ^{13}C NMR data show 1,2,33,41,42,50-$C_{60}H_6$ to be the main reaction product.[44,45]

¶ The results obtained[30] agree with the conclusion on the possible involvement of highly-dispersed nickel particles in the solid-phase hydrogenation of C_{60}.[23,24]



The hydrogen atoms in 1,2,33,41,42,50-$C_{60}H_6$ are not exchanged with deuterium atoms from D_2O on the NMR time scale, *i.e.*, the pK_a of $C_{60}H_6$ is much higher than that of $Bu^tC_{60}H$, which rapidly exchanges protons with the medium.[48] An attempt to isomerise 1,2,33,41,42,50-$C_{60}H_6$ in the presence of a Pd/C or Pt/C catalyst (as has been done for 7,8-$C_{70}H_2$, *cf.* Ref 49) resulted in rapid dehydrogenation of hydrofullerene instead of the expected reaction.[44]

The reaction in the $C_{70}-Zn/Cu-H_2O$ system under certain conditions results in preferential formation of $C_{70}H_{10}$, 7,8,19,26,33,37,45,49,53,63-$C_{70}H_{10}$ being the major isomer.[50] For various reasons (the presence of an oxide film, difficult separation of the products from the reaction mixture, *etc.*), efficient and selective reduction of fullerenes in the presence of other metals (Ti, Al, Mg)[44,46] was found to be impossible.

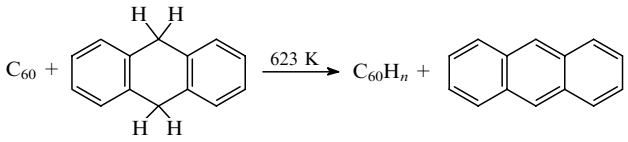
Water is the most suitable proton donor for the preparation of reduced fullerene derivatives in the $C_n-Zn/Cu-H_2O$ systems (n = 60, 70). Hydrofullerenes with low hydrogen content, *viz.*, $C_{60}H_2$, $C_{60}H_4$, $C_{60}H_6$ and $C_{70}H_{10}$, were obtained in good yields.[44,50] The isomer distribution is controlled by the reduction kinetics. The use of strong acids as proton donors for the reduction of fullerenes gives hydrofullerenes with higher hydrogen content.[51]

In toluene, the reduction of the fullerene cage in the $C_{61}H_2$ fulleroid in the presence of Zn/Cu occurs more slowly than that of fullerene,[52] but the reaction in *o*-dichlorobenzene occurs quite efficiently to give three isomeric compounds $C_{61}H_4$ which are light- and air-sensitive even at low temperatures. The reaction of sodium naphthalenide with C_{60} in THF gives 1,1′,2,2′-tetrahydro-bi[60]fulleren-1-yl $C_{120}H_2$ together with other products (including 1,2-dihydrofullerene).[53] Compound $C_{120}H_2$ is also formed upon hydrolysis of the salt $(Me_2NC_6H_4)_3C^+[C_{60}]^{-\bullet}$ obtained by the reduction of C_{60} with the crystal violet radical.[54]

The reaction of C_{60} with dilithiumacetylenide results in bis(hydrofullerenyl)acetylene $C_{122}H_2$ (yield 6.6%).[53] It should be noted that deprotonation of $C_{120}H_2$ is accompanied by fast dissociation of the transient C_{120}^{2-} dianion to the C_{60}^{-} monoanion, whereas deprotonation of $C_{122}H_2$ results in the C_{122}^{2-} dianion.[53]

3. Reduction of fullerenes by organic compounds

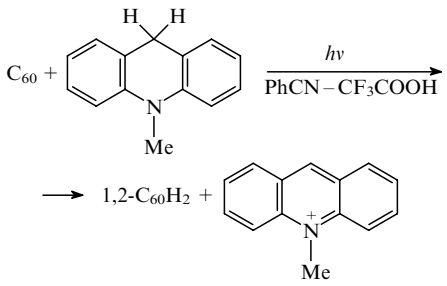
The reduction of fullerenes based on non-catalytic hydrogen transfer from a donor (*e.g.*, dihydroanthracene) to an acceptor (*e.g.*, C_{60} fullerene) results in selective formation of $C_{60}H_{36}$ † or $C_{60}H_{18}$, depending on the reaction conditions.[55,56]



The hydrogenation of C_{70} with dihydroanthracene results in a series of hydrofullerenes $C_{70}H_n$ (n = 36–46), $C_{70}H_{36}$ being the major product.

Anhydrous hydrazine in benzene reduces C_{60} and the endohedral compound $^3He@C_{60}$ into the lower hydrides $C_{60}H_2-C_{60}H_8$ and $^3He@C_{60}H_2-{}^3He@C_{60}H_8$; their compositions and structures were determined using ^1H and ^3He NMR spectroscopy (in the case of $^3He@C_{60}$). At high hydrazine concentrations, the reaction mixture also contained higher hydrofullerenes, *viz.*, $C_{60}H_{18}$ and $C_{60}H_{36}$.[57]

Photoinduced electron transfer (PET) plays an important role in the reduction and oxidation of fullerenes. Since the one-electron oxidation potential of the triplet-excited state of C_{60} is 1.14 V (relative to the saturated calomel electrode),[58] electron donors having less positive oxidation potentials can be used for the photoreduction of C_{60}. For example, the photoreduction of C_{60} with allyltributyltin in the presence of CF_3COOH results in the selective formation of 1-allyl-1,2-dihydrofullerene, C_{60}-1,2-(H)C_3H_5,[59] while the reaction of C_{60} with tributyltin hydride in benzene occurs (under irradiation[59] or at elevated temperatures[60]) to give C_{60}-1,2-(H)$SnBu_3$. If 10-methyl-9,10-dihydroacridine is used as a hydrogen donor in the presence of $PhCN-CF_3COOH$ in photoreduction of C_{60} (λ > 540 nm), fullerene is reduced selectively to give 1,2-$C_{60}H_2$ (70%).[59]

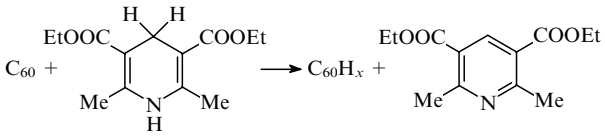


This photoreduction reaction of C_{60} is superior to, *e.g.*, the hydroboration of C_{60} (see Ref. 61) because of its selectivity and because mild reducing agents are used. However, in the absence of irradiation this reaction does not occur even at 373 K.

The bimolecular rate constant for quenching of the triplet-excited C_{60} ($^3C_{60}$) by 10-methyl-9,10-dihydroacridine (k_q = 4.3×10^9 litre mol^{-1} s^{-1}) and the mechanism of the photoreduction of C_{60} have been determined.[62]

Similarly to the two-electron reduction of C_{60} in the presence of 10-methyl-9,10-dihydroacridine, the one-electron reduction of C_{60} involving 1-benzyl-1,4-dihydronicotinamide and its dimer occurs through photoinduced electron transfer from the electron donor to $^3C_{60}$.[63,64] The difference between the redox and acid-base properties of the radical cations formed upon PET can define the reaction pathway.

Heating (100 °C, toluene) or pulse photolysis (Nd^{3+} : YAG laser, λ = 532 nm, benzonitrile) of a mixture of C_{60} with the Hantzsch ester (diethyl 2,6-dimethyl-1,4-dihydropyridine-3,5-dicarboxylate) under anaerobic conditions result in fullerene hydrogenation products and diethyl 2,6-dimethylpyridine-3,5-dicarboxylate (the dehydrogenation product of the Hantzsch ester).



The progress of the dehydrogenation of the Hantzsch ester with the fullerene was monitored by ^1H NMR spectroscopy and a signal at δ 5.93 characteristic of 1,2-$C_{60}H_2$ could be detected if the reaction was carried out at room temperature. Heating of the reaction mixture in the presence of excess Hantzsch ester results in hydrofullerenes with the composition $C_{60}H_x$ (x = 2, 4, 6) identified by mass spectrometry.[65,66]

Illumination of the same mixture by visible light under aerobic conditions (room temperature), in agreement with the known data[67] on the sensitising effect of C_{60}, completely converted the Hantzsch ester in the presence of fullerenes to give the correspond-

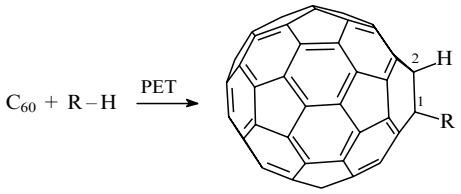
† Lobach *et al.*[56] paid much attention to standardisation of the conditions for the preparation of $C_{60}H_{36}$ because the synthetic procedure affects considerably the properties and structures of hydrofullerenes.

ing pyridine derivative; the concentration of C_{60} remained unchanged.[65]

Tertiary amines are widely used in the photoreduction of fullerenes. Prolonged irradiation (λ = 350 nm, N_2) of a mixture of C_{60} with tertiary amines $RNMe_2$ (R = Ph, Me) gives 1,2-$C_{60}H_2$ along with a pyrrolidine derivative of C_{60} (fullereno[C_{60}]pyrrolidine).[68]

The ESR method was used to study many photoreduction reactions of C_{60}. For example, it was found that the $C_{60}^{-\bullet}$ radical anion is formed in the presence of photo-activated TiO_2[69] or triethylamine[70] in a mixture of organic solvents[69,70] and in an aqueous solution.[71] The photochemical reduction of C_{60} in the presence of TiO_2 or ascorbic acid was studied.[72] It was found that the C_{60} fullerene is reduced photochemically by triethylamine to give $C_{60}^{-\bullet}$. Prolonged irradiation of the reaction mixture results in $C_{60}H^-$ (the C_{60}^{2-} protonation product) which is decomposed to $C_{60}^{-\bullet}$ in a dark reaction.[73]

Irradiation of C_{60} in the presence of certain acceptor-type photosensitisers (9,10-dicyanoanthracene, 1,4-dicyanonaphthalene, *N*-methylacridinium and 2,4,6-triphenylpyrylium hexafluorophosphates) results in 1-substituted 1,2-dihydro[60]fullerenes following introduction of proton donors such as *N*,*N*-dimethylformamide, 1,3-dioxolane, phenylacetaldehyde, methyl formate, *tert*-butyl alcohol, propionic acid, *etc*.[74,75]



Co-sensitisers, *e.g*., biphenyl, are used in order to increase the yield of the products. The $C_{60}^{+\bullet}$ radical cation formed was shown to possess electrophilic character.

$$C_{60} \xrightarrow[\text{PET}]{h\nu} C_{60}^{+\bullet},$$

$$C_{60}^{+\bullet} + RH \longrightarrow H-C_{60}^{+} + R^{\bullet},$$

$$H-C_{60}^{+} + R^{\bullet} + e^- \longrightarrow H-C_{60}-R.$$

4. Other methods for the preparation of hydrogen-containing fullerene derivatives

Dihydrofullerene $C_{60}H_2$ was obtained in low yield upon sonication of C_{60} solutions in decahydronaphthalene.[76] The formation of dihydrofullerene $C_{60}H_2$ upon electrochemical hydrogenation of C_{60} in 30% aqueous KOH was also reported.[77] The electrolytic hydrogenation of C_{60} and dehydrogenation of $C_{60}H_2$ are reversible.[77]

$$C_{60} + xH_2O + x\,e^- \rightleftharpoons C_{60}H_x + xOH^-.$$

Mechanochemical reactions involving fullerenes and graphite have been studied.[78–81] Mechanochemical treatment of graphite in an atmosphere of hydrogen (1 MPa) at room temperature results in nano-structured graphite which adsorbs hydrogen both physically and chemically.[81] The method of 'high-speed vibration milling' (under these conditions, crystalline C_{60} is pulverised into particles with sizes smaller than 1 μm) was found to be highly efficient for the supramolecular complexation of fullerenes and their derivatives with γ-cyclodextrin and sulfocalixarene.[79] The yields of [4 + 2]-cycloaddition products of fused aromatic compounds (anthracene, tetracene, pentacene and naphtho[2,3-*a*]pyrene) to C_{60} obtained according to this procedure are higher than the yields of the same products obtained by heating the components in solution.[80] The solid-phase reaction of C_{60} with KCN, unlike the homogeneous reaction, gives the C_{120} dimer.[82] This reaction also occurs in the presence of other salts (K_2CO_3, AcOK), metals (Li, Na, K, Mg, Al and Zn) and organic bases (4-dimethylamino- and 4-aminopyridine).[82] It is probable that the mechanochemical method can also be applied for the synthesis of hydrogenated fullerene derivatives ‡ (similarly to the hydrogenation of organic compounds with hydrogen[84]).

III. Properties of hydrofullerenes

1. The state of hydrogen in solid hydrofullerenes

In the majority of experiments on the reduction of C_{60} and C_{70}, mixtures of fullerene hydrides are obtained. Solid samples of hydrofullerenes with the same molecular formula but prepared by different methods differ strongly in their solubilities, light and air resistances, abilities to withstand prolonged storage and in other properties (see, *e.g*., Refs 13, 51, 85).

Of hydrofullerenes, $C_{60}H_{36}$ has been studied most thoroughly. Electron-impact and field-desorption mass spectrometric analysis showed that $C_{60}H_{18}$ is the first stable thermal decomposition product of $C_{60}H_{36}$ prepared under the conditions of non-catalytic transfer of hydrogen from a donor to an acceptor.[56] The intermediate hydrides $C_{60}H_n$ (n = 33–35) are much less stable than $C_{60}H_{36}$. Intense peaks of $C_{60}H_{18}$ and C_{60} appearing in the mass spectrum of a sample of $C_{60}H_{36}$ after its prolonged storage indicate that $C_{60}H_{36}$ undergoes decomposition; the presence of the C_{60} peak is evidence of possible reversible addition of hydrogen to fullerene. The formation of $C_{60}H_{36}$ as the only reduction product of C_{60} under non-catalytic hydrogen transfer conditions is also confirmed by the spectra obtained using matrix-assisted laser desorption ionisation mass spectrometry (MALDI-MS): the most abundant peak is that of $C_{60}H_{35}^+$, the fragmentation is insignificant, the intensities of the satellite peaks corresponding to the oxidation products $C_{60}H_xO^+$ are much lower than in the case of the $C_{60}H_{36}$ obtained by the Birch reduction.[39]

As noted above, solid hydrofullerenes decompose at temperatures above 800 K in an inert or in a hydrogen atmosphere to give hydrogen and fullerenes.[23,86] The thermal decomposition product of crystalline $C_{60}D_{24}$ at 823 K mainly consists of fullerene (Fig. 3)

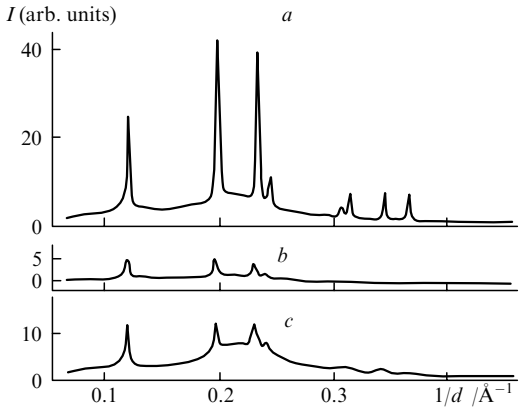


Figure 3. Diffractograms of the parent fullerene (*a*), fullerene deuteride $C_{60}D_{24}$ (*b*) and the product of thermodecomposition of the deuteride (*c*).[25]

with the distance between the C_{60} molecules considerably exceeding that in the parent fullerene (the a_0 constants of the FCC lattice of the decomposition product and C_{60} are 1.452 and 1.417 nm, respectively). Presumably, the increase in the fullerene crystal lattice constant resulting from hydrofullerene decomposition can be useful in the synthesis of alkali metal fullerides with superconducting properties.[86] The position of the C1*s* peak maximum in the X-ray photoelectron spectrum of the $C_{60}D_{24}$ deuteride is shifted towards lower bond energies in comparison with that of C_{60}, which makes it possible to conclude that a small positive charge exists on the deuterium atoms. The peak becomes narrower

‡ Apparently, the microwave irradiation method[83] can also be used for the preparation of hydrogenated fullerene derivatives.

as the deuteride undergoes thermal decomposition, and its 'centre of gravity' shifts to higher bond energies.[86]

Particular interest in the fundamental and applied aspects is felt in the synthesis of hydrofullerenes in which the hydrogen atoms are located both outside and inside the fullerene cage. This is a way to increase the hydrogen capacity of fullerenes. Therefore, studies of the properties of individual hydrogen molecules located in a closed space are also of interest. For example, it was found that compounds $C_{60}H_{52}$ and $C_{60}H_{48}$ fluoresce in the long-wave region. This phenomenon was interpreted taking account of the possibility of penetration of hydrogen molecules into a closed hydrofullerene cavity.[87] Hydrofullerites obtained under ultrahigh hydrogen pressures, $p_{H_2} = 0.6$ and 3.0 GPa, were studied by inelastic neutron scattering (INS) spectroscopy.[88] The spectra showed that the synthesis of $C_{60}H_x$ ($p_{H_2} = 0.6$ and 3.0 GPa, 620 K, 24 h) followed by cooling the sample to 77 K under a high pressure of H_2 is accompanied by the formation of a solid solution of hydrogen in the $C_{60}H_x$ lattice ($x \approx 24$ and 32–46 for $p_{H_2} = 0.6$ and 3.0 GPa, respectively).[88,89] The main features of the INS spectrum of $C_{60}H_{32}$ obtained at $p_{H_2} = 3.0$ GPa [90] are similar to those for $C_{60}H_{\sim 23}$ obtained at $p_{H_2} = 0.6$ GPa.[91] Presumably, a considerable fraction of hydrogen (~ 3 H_2 molecules per C_{60} molecule) are located as H_2 molecules in the interstices of the $C_{60}H_x$ lattices. Upon heating to 293 K, the H_2 molecules leave the sample with heat evolution. Dissolved molecular hydrogen is detected by the rotational transition peaks in the H_2 molecule (~ 15 and 30 meV) in the difference INS spectra between the 'quenched' (H_2-containing) and heated (H_2-free) products. The possibility of polymeric binding of the $C_{60}H_{32}$ hydrofullerite at high H_2 pressure (3.0 GPa) is suggested by the presence of a peak near 13 meV in its INS spectrum. The low-energy part of the INS spectrum (< 9 meV) for $C_{60}H_{32}$ is believed to indicate [88,89] the presence of an endohedral hydrogen atom unbound with carbon.

Hydrofullerites obtained at $p_{H_2} = 0.6$ and 3.0 GPa and $T = 520$–620 K and then quenched at $T < 120$ K exhibited ferromagnetic properties up to $T \approx 300$ K. Their magnetisation was as high as $M = 1.2$ emu g^{-1} at $H = 1$ T.[92] According to analytical data, the concentration of ferromagnetic admixtures in hydrofullerenes is insignificant. Magnetisation which disappears upon heating of the samples above 340 K or upon prolonged storage at room temperature is a property inherent in hydrofullerites obtained by various methods.[92,93] Probably, their magnetisation is caused by the presence of unstable transient radical-type electronic states. The penetration of hydrogen inside the cage, polymerisation of the fullerene cages upon dehydrogenation and other high-energy transformations of the C–C and C–H bonds in sterically hindered fullerene lattices could be the reasons for the generation of quasistable carbon atoms with unsaturated valence or delocalised unpaired electrons.

2. Thermodynamic analysis of the dehydrogenation of hydrofullerenes

The thermodynamic properties of the $C_{60}H_{36}$ hydrofullerene obtained by non-catalytic hydrogen transfer [56] have been studied in the temperature range from 4.8 to 340 K.[94,95] The following values of thermal capacity, enthalpy, entropy and Gibbs free energy were found for the hydrofullerene obtained at $T = 298.15$ K and $p = 101.325$ kPa:

$$C_p^\circ(298.15) = 690 \text{ J K}^{-1} \text{ mol}^{-1};$$

$$H^\circ(298.15) - H^\circ(0) = 84.94 \text{ kJ mol}^{-1};$$

$$S^\circ(298.15) = 506 \text{ J K}^{-1} \text{ mol}^{-1};$$

$$-[G^\circ(298.15) - H^\circ(0)] = 66.17 \text{ kJ mol}^{-1}.$$

High temperature is required for the dehydrogenation of hydrogen-containing fullerene derivatives. Quantum-chemical calculations of the C–H bond energy in fullerene hydrides performed by the semi-empirical AM1 method gave the values of 306.27, 298.32, 295.80 and 293.72 kJ mol^{-1} for $C_{60}H_{12}$ (T_h), $C_{60}H_{18}$ (C_3) and $C_{60}H_{36}$ (T and T_h), respectively.[96] Heating of $C_{60}H_{36}$ under isothermal conditions (594 and 610 K, 20 h) results in dehydrogenation of the sample and evolution of gaseous H_2. In this case, the composition of the solid residue is '$C_{60}H_6$': $C_{60}H_{36} \rightarrow C_{60}H_{18} \rightarrow$ '$C_{60}H_6$'. The dehydrogenation occurs stepwise [97] and is accompanied by sublimation of $C_{60}H_{36}$ and $C_{60}H_{18}$. The estimated saturated vapour pressures of $C_{60}H_{36}$ and $C_{60}H_{18}$ at 594 K are 9.8×10^{-9} and 5.4×10^{-9} MPa, respectively.

3. Specific features of hydrofullerene structures

The $C_{60}D_{24}$ deuteride obtained by deuteration of crystalline fullerene with gaseous D_2 is a crystalline powder with an FCC lattice ($a_0 = 1.455$ nm) [23] and a crystallite size of 51–56 nm.[25] The synthesis of $C_{60}D_{36}$ with an FCC lattice ($a_0 = 1.500$ nm) has been reported.[27] On the other hand, $C_{60}H_{36}$ samples obtained by hydrogenation under high pressure [98] or in the presence of iodine [99] have body-centred cubic (BCC) lattices.[100]

Theoretical and experimental studies of the structures of the most stable (T, T_h, S_6 and two D_{3d}) isomers of the $C_{60}H_{36}$ hydrofullerene have been carried out.[99–103] Comparison of the experimental ^1H and ^{13}C NMR spectra of the solid $C_{60}H_{36}$ (see Ref. 99) with the calculated ones [104] made it possible to assume a structure with the T symmetry [105] for $C_{60}H_{36}$ obtained by non-catalytic hydrogen transfer.[56] According to X-ray emission and photoelectron spectral data, quantum-chemical calculations and electrochemical behaviour, the most probable structure for the $C_{60}H_{36}$ hydrofullerene is that with the T symmetry and with four isolated benzenoid (non-hydrogenated) rings located on the surface of the $C_{60}H_{36}$ hydrofullerene in the vertices of an imaginary tetrahedron (Fig. 4).[103,106,107]

Comparison of the CK_α spectra of C_{60}, $C_{60}H_{36}$ and C_6H_6 prompts the conclusion that the π-electron systems of hydrofullerenes and benzene are similar; the localisation of the HOMO electron density of the $C_{60}H_{36}$ hydrofullerene on the benzenoid rings allows one to assume that η^6 metal complexes based on $C_{60}H_{36}$ can be synthesised.[106,108] Studies of the electrochemical behaviour of the $C_{60}H_{36}$ hydrofullerene indicates that $C_{60}H_{36}$ is a rather 'hard' molecule with low reactivity in redox reactions. The electrochemical electronegativity decreases in the series $C_{60} > C_{60}H_2 > C_{60}H_{36} \approx C_6H_6$. The approximate equivalence of the electronegativities of the two latter compounds can also be evidence in favour of the T-symmetrical structure of $C_{60}H_{36}$.[107]

The presence of a large number of reaction centres in the fullerene molecules results in a large number of possible isomers of hydro- and fluorofullerenes. Based on a combination of the MO LCAO method with molecular mechanics, Breslavskaya and D'yachkov [109] predicted the structures of the most stable C_nX_k

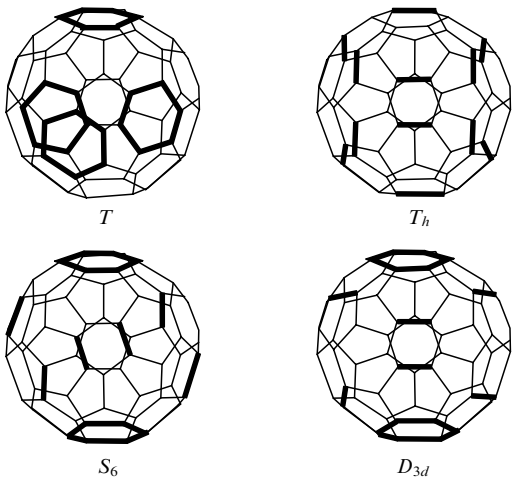


Figure 4. The most stable $C_{60}H_{36}$ isomers (one of the two D_{3d} is shown).[103] The thick lines denote the non-hydrogenated C–C bonds.

isomers with high hydrogen and fluorine contents (X = H, F; $n = 76$, 78, 84) and compared the theoretical data with the available experimental results. According to the neutron diffraction structural data[110] for $C_{60}D_{36}$ prepared according to a reported method[99] by deuteration of C_{60} at 623 K and a D_2 pressure of 3.4 MPa in the presence of iodine as a promoter, the structure with the *T* symmetry is most stable for this deuteriofullerene as well [a structure with the *T* symmetry has been suggested previously[99] as the most stable one for $C_{60}H_{36}$ (IR and ^{13}C NMR spectral data)].

Billups *et al.*[111] studied the ^3He spectra of $^3He@C_{60}H_{36}$ samples prepared by reduction of $^3He@C_{60}$ with lithium in liquid ammonia[38] and by non-catalytic hydrogen transfer.[55] The ^3He NMR spectra of both $^3He@C_{60}H_{36}$ samples contain peaks at δ −7.7 and −7.8; the third peak at δ −16.45 was assigned to the chemical shift of the $^3He@C_{60}H_{18}$ hydrofullerene. Comparison of the experimental spectra[111] with the calculated chemical shifts for the most stable $^3He@C_{60}H_{36}$ isomers [δ −10.8 (*T*), −7.7 ($D_{3d'}$), −6.1 (S_6), −3.4 (T_h) and −5.6 (D_{3d})][104] makes it possible to assume that the $D_{3d'}$ isomer is formed in both cases. In addition, based on the ^3He NMR spectra of the sample prepared by reduction of $^3He@C_{60}$ with lithium in liquid ammonia, the conclusion was made as to the low probability of the formation of the isomer with the T_h symmetry which had previously been suggested[38] for a $^3He@C_{60}H_{36}$ sample. According to the reported data,[112] the isomer with the S_6 symmetry (see Fig. 4) is the most stable $C_{60}H_{36}$ hydride, though the difference between the energies of the ten most stable isomers is less than 62.76 kJ mol^{-1}. In the previous studies by the same authors, isomers with the *T* and D_{3d} symmetries were noted as the most stable ones of the large number of possible structures suggested for the $C_{60}H_{36}$ fullerene hydride.[101]

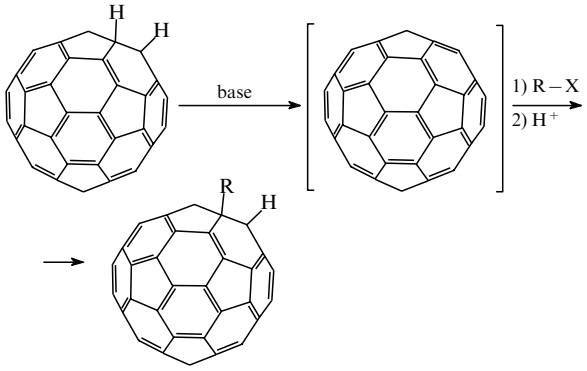
Thus, it has been shown for $C_{60}H_{36}$ that not only different chemical methods can result in isomers with different symmetries, but also products with different isomer compositions can be formed within a single procedure (see, *e.g.*, Refs 85 and 106). In the case of the $C_{60}H_{36}$ molecule, the problem of the most stable structure remains open and requires more accurate theoretical calculations. It is quite possible that certain methods for the synthesis of $C_{60}H_{36}$ can produce thermodynamically unstable isomers (*e.g.*, due to kinetic factors). In order to verify the validity of this assumption, one has to perform in-depth experimental and theoretical studies, including the isomerisation of $C_{60}H_{36}$. A reliable determination of the $C_{60}H_{36}$ structure is also interesting from the practical respect. For instance, the knowledge of its exact structure is very useful when one plans the syntheses based on this hydrofullerene.

4. The reactivities of hydrofullerenes

According to the reported data,[113] a hydride with the net composition $C_{60}H_{18.7}$ with $a_0 = 1.476$ nm is stable up to 703 K in an Ar atmosphere. Further increase in the temperature results in hydrogen evolution and is accompanied by decomposition of part of the fullerene molecules and formation of graphite platelets and methane.§ The use of catalytic amounts of ruthenium or platinum did not decrease the temperature of hydrofullerene dehydrogenation.

The dehydrogenation of $C_{60}H_{36}$ on treatment with a strong hydrogen acceptor, *viz.*, 2,3-dichloro-5,6-dicyano-1,4-benzoquinone, which is widely used in the analysis of hydrofullerenes, was found to be non-quantitative, since in addition to C_{60}, its derivatives were also formed.[56] Thermogravimetric (TG) and differential thermogravimetric (DTG) studies of $C_{60}H_{36}$ in the presence of oxygen were carried out.[30] It was found that $C_{60}H_{36}$ is partially oxidised at 550 K to give $C_{60}H_{36}O_x$ ($x \approx 4.8$) and that its combustion occurs at 745 K. As it might have been expected, these temperatures are much lower than the temperatures of partial oxidation and combustion of C_{60} (705 and 888 K, respectively).[30] Complexes of polyaromatic compounds and fullerene with platinum immobilised on silica exist in the temperature range 323–373 K and can be repeatedly hydrogenated and dehydrogenated.[114] It is these properties that are required for practically usable systems for the storage of hydrogen: good reproducibility of hydrogenation–dehydrogenation cycles in a temperature range as low as possible.

Deprotonation of 1,2-$C_{60}H_2$ in the presence of Bu_4NOH (benzonitrile, anaerobic conditions) is accompanied by the formation of the C_{60}^{2-} dianion which quickly reacts with a number of alkyl halides to give mono- and dialkylfullerenes.[115]



Ph_2CHBr, $PhCH_2Br$, MeI, propargyl bromide and allyl bromide are used as the alkylating reagents. However, attempts at alkylation of the C_{60}^{2-} formed with octyl bromide failed. Analysis of the absorption spectra for mono- and dialkylated C_{60} derivatives shows that the sp^3 carbon atoms in the monoalkyl derivative are in the 1,2-position, while in dialkyl-C_{60} derivatives, they are in the 1,4-position. Fukuzumi *et al.*[116] studied the mechanisms of formation of R_2C_{60} and $R(R')C_{60}$ dialkylfullerenes from chemically obtained C_{60}^{2-} and various alkyl halides (RX and R′X) differing both in the nature of the R and R′ radicals and of the halogen atom. In the first step, transfer of one electron from the C_{60}^{2-} dianion to an alkyl halide occurs to give RC_{60}^-, which is transformed to R_2C_{60} or $R(R')C_{60}$ according to the S_N2 mechanism.

It was shown that protonation of $Bu^tC_{60}^-$ with trifluoroacetic acid initially gives 1,4-$Bu^tC_{60}H$; the latter is then quickly transformed to 1,2-$Bu^tC_{60}H$ which is more stable thermodynamically. Photoinduced transfer of an electron from a soft reducing agent, 1-benzyl-4-*tert*-butyl-1,4-dihydronicotinamide, to triplet-excited C_{60} results eventually in selective two-electron reduction of C_{60} to give $Bu^tC_{60}^-$, which reacts with $PhCH_2Br$ or Bu^tI in the next step to give 1,4-$Bu^t(PhCH_2)C_{60}$ (see Ref. 63) or $Bu_2^tC_{60}$ (see Ref. 117), respectively. Photoalkylation of C_{70} occurs similarly to give $Bu^tC_{70}^-$ (and $Bu^tC_{70}H$ after protonation); the formation of five regioisomers is possible for $Bu^tC_{70}^-$, unlike $AlkC_{60}^-$ which gives only one product.[118]

The reactivities of the $C_{60}^{-\bullet}$ radical anion or the C_{60}^{2-} dianion manifest themselves not only in reactions with alkyl halides. The higher C–H bond strength in lower hydrofullerenes in comparison with the higher ones results in the possibility of the transfer of a hydrogen atom onto these anions from higher hydrofullerenes. It was shown by cyclic voltammetry that the reaction between C_{60} and $C_{60}H_{36}$ in a propylene carbonate–toluene mixture is induced by electron transfer and eventually involves transfer of a hydrogen atom from $C_{60}H_{36}$ to the fullerene.[119] The pathway according to which the $C_{60}^{-\bullet}$ radical anion and the C_{60}^{2-} dianion electrogenerated from C_{60} react with $C_{60}H_{36}$ was considered as the most probable variant of the transformation; this reaction involves the transfer of a hydrogen atom from $C_{60}H_{36}$ and results in $C_{60}H_2$ (proton transfer is impossible since the calculated[120] pK_1 for $C_{60}H_{36}$ is 31.35 and $C_{60}H_2$ is a rather strong acid[121,122] with $pK_1 = 4.7$ and $pK_2 = 16$). In order to estimate the possibility of formation of

§ Presumably, the character of thermal decomposition and the crystal lattice parameters of hydrofullerenes depend considerably on the conditions of fullerene hydrogenation.

$C_{60}H_2$ from C_{60} and $C_{60}H_{36}$, Tkachenko *et al.*[119] calculated the mean C–H bond energies in hydrofullerenes $C_{60}H_2$ and $C_{60}H_{36}$, which were found to be 295 and 279 kJ mol^{-1}, respectively. Thus, cleavage of a C–H bond in $C_{60}H_{36}$ with subsequent formation of a C–H bond in $C_{60}H_2$ is energetically favourable.

The relatively week C–H bond strength in higher hydrofullerenes enables its homolytic cleavage by other relatively weak acceptors as well. Elimination of a hydrogen atom from $C_{60}H_{36}$ under mild conditions can also be carried out by treatment with the 2-(*p*-fluorophenyl)hexafluoroisopropyl radical.[123] Heating (353 K) of hydrofullerenes $C_{60}H_x$ ($x = 6-18$) with $Hg[N(SiMe_3)_2]_2$, $Ti[N(SiMe_3)_2](NEt_2)_3$ and other metal complexes also results in elimination of a hydrogen atom from $C_{60}H_x$ and formation of fullerene-containing oligomers, *e.g.*, $-[(C_{60}H_n)Hg_2]_m-$.[124]

$$mC_{60}H_x + 2mHg[N(SiMe_3)_2]_2 \longrightarrow$$
$$\longrightarrow -[(C_{60}H_n)Hg_2]_m- + 2mHN(SiMe_3)_2.$$

IV. Sorption of hydrogen by carbon nanotubes and graphite nanofibres

Much attention has been given recently to the sorption of hydrogen by such carbon nanostructures as carbon nanotubes, graphite nanofibres and their metal-doped modifications.

Carbon nanotubes (NT) with low-defect structures were found in 1991 in the products of electric-arc evaporation of graphite.[125] However, long before that, similar NT¶ with a high content of structural defects have repeatedly been detected in solid products of hydrocarbon pyrolysis on metal catalysts.[126] Owing to its high efficiency, the catalytic pyrolysis of hydrocarbons is still widely used for the practical production of long (up to millimetres) carbon nanostructures, including NT and the so-called vapour-grown carbon fibres (VGCF).

A graphene sheet rolled in a seamless cylinder is the main element of carbon NT. Multi-walled nanotubes (MWNT) consisting of graphene sheets rolled as a cylindrical spiral also exist.

Vapour-grown carbon nanofibres can consist of parallel-sided graphene platelets perpendicular to the fibre axis (platelet-type VGCF), of nested graphene cones (herring-bone VGCF), of truncated cones (conical layer nanotubes, CLNT), *etc*.

Single-walled nanotubes (SWNT) are closed networks built of quasi-sp^2-hybridised carbon atoms. The network consists of hexagonal cells on the side surface of the cylinder. Open and closed SWNT exist; in the latter, the cylinder ends are closed by hemispheres ('fullerene halves') consisting of hexagonal and pentagonal cells. The SWNT diameter ranges within 0.8–5 nm (most often, 1–2 nm) and its length is 1–500 μm (most often, 5–50 μm). Carbon SWNT have a rather narrow diameter distribution, in contrast to activated carbons in which the sizes of macro-, meso- and micropores differ by a factor of several hundred.[127]

A typical feature of SWNT is the formation of rather strong molecular aggregates (named as bundles, strands, ropes, braids, *etc*.), in which the axes of separate SWNT are parallel to each other. The shortest distance between the carbon skeletons of the adjacent SWNT in the bundles is 0.32 nm. This value is close to the size of the van der Waals distance between graphene layers in graphite and can be changed by introduction of inorganic or organic intercalants, surfactants or by chemical modification of the cylindrical surface of the NT.

Ideal (defect-free) multi-walled nanotubes (MWNT) are built of SWNT inserted one into another. Ideal MWNT are formed in a carbon arc if no metal catalyst is added to the graphite to be vaporised. The distances between the layers in MWNT are close to the interlayer distance in graphite. The outer diameters of electric-arc MWNT are 5–40 nm (most often 15 nm), the inner diameters are 0.8–5.0 nm (mostly 1–2 nm), and the lengths are 0.5–70 μm.

¶ These nanotubes were called tubular graphite fibres.

The synthesis of SWNT and MWNT is accompanied by the formation of other carbon modifications: fullerenes, multilayer polyhedral nanoparticles, graphite microcrystals and amorphous carbon. Furthermore, mixtures of products obtained by the catalytic method contain metal particles. The content of carbon NT in the synthesis products does not exceed 20%–70% (for different methods), therefore in all cases purification from admixtures is the most laborious stage in the preparation of pure carbon NT.

Many publications (see, *e.g.*, the corresponding reviews[128–133]) report the state-of-the-art of the methods for the preparation and study of the properties of carbon nanostructures and their use.

1. Sorption of hydrogen by single-walled carbon nanotubes

The carbon material obtained by the electric-arc method and containing single-walled carbon NT (in the form of bundles containing 7–14 NT), amorphous carbon and particles of a catalyst (for example, Co) adsorbs 5 mass %–10 mass % H_2 (with respect to the pure SWNT) at 273 K and 300 Torr followed by cooling to 90 K.[134] According to the temperature-programmed desorption (TPD) data,[134] hydrogen is desorbed from nanotubes and activated carbon at 133 K. However, if a sample containing SWNT is preliminarily subjected to a treatment which opens the 'plugs' at the tube ends, a second peak almost at room temperature (290 K) appears on the TPD curve. This peak is explained by the evolution of hydrogen adsorbed inside the SWNT due to the penetration of H_2 molecules through the open tube ends. No high-temperature peak of this type is observed in the desorption of hydrogen from activated carbon samples or from fullerene soot obtained in the absence of a catalyst. It is believed[134] that in the carbon material obtained by the electric-arc method, the 'high-temperature' hydrogen is mainly located in the SWNT channels, whereas the 'low-temperature' hydrogen is adsorbed on amorphous carbon, on the outer surface of the SWNT and/or in the intertube space of the SWNT bundles.

The amount of adsorbed hydrogen (99.9999% purity) for relatively pure carbon SWNT obtained by the laser method (see Refs 135 and 136) exceeds 8 mass % H_2 at 10–12 MPa and 80 K.[137] In this case, the mean diameter and the specific surface of a separate SWNT are ~ 1.3 nm and 1300 $m^2\ g^{-1}$, respectively. The diameters of the SWNT bundles are ~ 6–12 nm. The outer specific surface of the bundles measured by the BET method is 285±5 $m^2\ g^{-1}$. The amount of adsorbed hydrogen depends on the number of 'sorption–desorption' cycles. For freshly prepared samples of pure SWNT, the C : H ratio of ≈ 1 (~ 8.25 mass % H_2) is achieved at 80 K and 7 MPa of H_2 (Fig. 5, curve *1*).

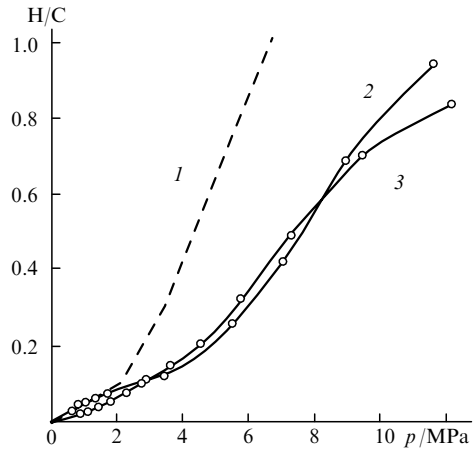


Figure 5. Dependence of the amount of hydrogen adsorbed by an SWNT at 80 K on pressure in the first (*1*) and subsequent cycles (*2* and *3*).[137]

Hydrogen is initially adsorbed on the outer surface of an SWNT bundle. An increase in pressure to 12 MPa during subsequent cycles increases the amount of absorbed H_2, which is attributed to the penetration of H_2 molecules into the intertube space of the bundles. As a result, the intertube space increases and the bundle breaks into separate SWNT; the outer SWNT surfaces are completely covered and the inner surfaces are partially covered by H_2 molecules (Fig. 5). The increase in the intertube distance inside the SWNT bundle can be detected by X-ray diffraction and NMR spectroscopy.[138] It has been shown that an SWNT bundle expands after immersing a carbon SWNT sample in a nitric acid solution and shrinks to the original configuration after deintercalation of HNO_3, *i.e.*, this change is reversible.

Liu *et al.*[139] synthesised carbon SWNT by the electric arc method (the production rate of SWNT was 2 g per hour) in the presence of hydrogen [a nickel–cobalt–iron powder (Ni : Co : Fe = 3 : 0.75 : 0.75) was used as the catalyst, and FeS was used as the SWNT growth accelerator]. The content of SWNT in the carbon material obtained by this method was ~ 60%, the mean SWNT size was 1.85 nm, the diameter of the SWNT bundles was about 20 nm. Upon treatment of the SWNT samples, which included, in particular, heating at 770 K, the amount of adsorbed hydrogen (room temperature, 10 MPa) reached 4.2 mass %, which corresponded to the ratio H : C = 0.52. Up to 78% of the adsorbed hydrogen desorbed under standard conditions. The remaining hydrogen (from 0.52 mass % to 0.95 mass % H_2 for different SWNT specimens) desorbed on heating the sample to 423 K.

Studies of the hydrogen-sorbing properties of a carbon material obtained by the electric-arc method [140] and containing ~ 70 mass % SWNT showed that it adsorbs about 3.5 mass % H_2 at 10 MPa and with multiple repetition of the cycles 'cooling to 77 K – heating to 300 K'.[3, 6] Interesting results were reported [141] that up to 6.5 mass % – 7.0 mass % of hydrogen was absorbed by an SWNT at room temperature and 0.1 MPa.

The specific surface and the gas-sorbing capacity of carbon materials depend considerably on the preliminary thermal treatment. It was shown [142] that heating of an SWNT sample, which has preliminarily been acid-etched, above 600 K *in vacuo* results in the liberation of different gases (CH_4, CO, CO_2 and H_2). After thermal pretreatment, SWNT adsorb a considerably greater amount of xenon at 95 K: the SWNT samples annealed at 1073 K absorbed 20 times more Xe than the samples heated to 623 K. The increase in the adsorption capacity of SWNT was explained by the effect of high-temperature annealing, which removes the carboxyl groups blocking the ends and defects of the NT walls (Fig. 6). Apparently, such a thermal treatment should also affect the hydrogen adsorption capacity of NT.

Hydrogen can also be stored in SWNT using an electrochemical process which is reversible. The relatively low but quite reliably measured hydrogen capacity in the process

$$HT + x\,H_2O + x\,e^- \xrightarrow{\text{charge}} (HT + x\,H) + x\,OH^-$$

is about 0.4 mass % for a number of SWNT specimens. In this case, SWNT/Au is the negative electrode, Ni is the positive electrode, $Hg/HgO/OH^-$ is the reference electrode, and 6 M KOH is the electrolyte. The capacity decreases by only 30% after 100 charge–discharge cycles.[143]

The maximum content of hydrogen in carbon NT specimens reduced with dihydroanthracene at 623 K or with lithium under modified Birch conditions corresponds to the '$C_9H-C_{10}H$' and 'C_8H' compositions, respectively;[144, 145] this is several times less than in the systems using physical hydrogen adsorption at high pressures. The desorption of hydrogen from such hydrogen-containing nanotube derivatives occurs only at 773 K, which implies that hydrogen is chemically bound.[145]

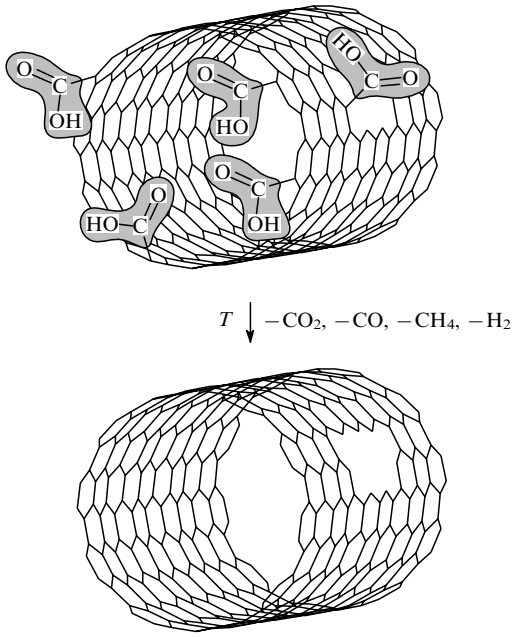


Figure 6. Schematic drawing of chemically treated single-walled NT before and after heating above 600 K.[142]

2. Sorption of hydrogen by graphite nanofibres

Inconsistent data on the hydrogen-sorbing properties have been reported for vapour-grown carbon fibres (VGCF). The highest hydrogen-sorbing capacity of VGCF (11 mass % – 67 mass % H_2) has been reported by Chambers *et al.*[146] The graphite nanofibres were obtained by catalytic pyrolysis of carbon-containing gases on the nanoparticles of a metal catalyst containing iron, nickel and copper, and then purified from the catalyst particles. The VGCF with a length of 10 – 100 μm and a diameter of 3 – 50 nm obtained by this method can be assigned to the platelet-type or conical layered structures.[146] In a favourable conformation, the distance between the graphene sheets is 0.337 nm, while the gas-kinetic molecular diameter of hydrogen is 0.289 nm. The sorption of hydrogen at 12 MPa and 298 K was studied on a Sieverts-type apparatus.

In a series of studies,[147, 148] attention was drawn to the necessity of careful preparation of the samples intended for the H_2 sorption capacity measurements. It was noted that VGCF having developed systems of slit-shaped nanopores with a great number of open edges have a perfect configuration for hydrogen adsorption. Owing to this unique VGCF structure, the hydrogen molecules interact not only with the graphene sheet surface but also with the adjacent H_2 molecules; it is believed that this may result in the capillary condensation of hydrogen at anomalously high temperatures.[146] Moreover, the sorption of H_2 is accompanied by the expansion of pores (crevices), which can also result in polymolecular sorption of hydrogen. Comparison of X-ray diffraction spectra of VGCF samples before and after hydrogen adsorption indicates that the interlayer distance d between separate graphene sheets increases to 0.347 nm after H_2 adsorption (d = 0.340 nm for the initial VGCF). As the adsorbed H_2 is removed from the sample, the parameter d returns to the original value (0.340 nm).[147, 148]

The results on the hydrogen sorption by VGCF reported by Chambers *et al.*[146] have evoked both much interest and many critical comments,† as all attempts to reproduce this experiment failed.[6, 149, 150] Moreover, the reported high values of H_2 absorption considerably exceed even the highest theoretical estimates.[2, 151]

† It may well be that an error was made in the evaluation of the amount of hydrogen adsorbed by the VGCF. For example, the same study [146] reported data on the sorption of hydrogen by palladium and intermetallic compounds which were much higher than the generally accepted values.

Stöbel *et al.*[150] studied the adsorption of hydrogen on two types of carbon materials: on various specimens of amorphous high-porosity activated carbon and on VGCF synthesised in the presence of a catalyst. The adsorption of H_2 by activated carbon measured at 296 K and an H_2 pressure of 12 MPa was 1.6 mass %, which is in good conformity with calculations on the physical adsorption of hydrogen. Under these conditions, the adsorption of H_2 by VGCF did not exceed 1.2 mass %. The authors [150] did not obtain high H_2 absorption on carbon nanofibres with parallel-laminated structure prepared by them; however, they noted an unusual behaviour of the material in a hydrogen atmosphere, which may be due to the fibre nanostructure.

The hydrogen-sorbing properties of a lithium- and potassium-doped carbon material prepared by catalytic decomposition of methane have been studied. After removal of the catalyst, the material contained up to 90% VGCF ‡ with an outer diameter of 25–35 nm, with mainly platelet or conical-layered structures.[152] Doping with lithium or potassium [Li(K) : C ≈ 1 : 15] occurred under conditions of the solid-phase reaction between VGCF and Li(K)-containing compounds such as carbonates and nitrates. Hydrogen uptake reaches 20 mass % for the Li-containing VGCF at 653 K and 14 mass % for the K-containing VGCF at room temperature, which amounts to ~ 160 and 112 kg (H_2) m^{-3}, respectively.[152] Multiple repetition of the H_2 absorption–desorption process results in an insignificant (~ 10%) loss of the sorption capacity of the material. The specimens doped with lithium had higher chemical stabilities under ordinary conditions than those doped with potassium. The high sorption capacity of Li(K)-doped VGCF is attributed to the layered VGCF structure with large interlayer clearance (0.347 and 0.335 nm for VGCF and graphite, respectively) between the small-size (50 nm and less) graphene sheets in the VGCF, as well as to the presence of an alkali metal. Without alkali doping, the absorption of H_2 by the VGCF decreases abruptly.

Chen *et al.*[152] have also obtained anomalously high values of H_2 sorption by graphite doped with Li and K [up to 35%–70% of the sorption capacity of Li(K)-VGCF at 473–673 K and p_{H_2} = 0.1 MPa]. The high hydrogen sorption by VGCF doped with alkali metals was explained by possible dissociative hydrogenation of the carbon sorbent, in which the alkali metal is a catalytic active centre. This hypothesis is supported by the fact that a band characteristic of the Li–H bond vibrations (~ 1420 cm^{-1}) appears in the IR spectrum of a Li-doped VGCF specimen upon treatment with H_2. In the temperature range from 473 to 673 K, the intensity of the Li–H vibrations correlates with the hydrogen absorption. Subsequently, the hydrogen atoms are transferred to the carbon network and add to carbon atoms. The appearance of an absorption band in the region of the C–H stretching vibrations confirms the dissociative mechanism of VGCF interaction with hydrogen. An increase in temperature causes the desorption of hydrogen and, correspondingly, disappearance of the bands assigned to vibrations of the C–H bond. Thus, systems based on Li(K)-VGCF can store hydrogen at elevated temperatures.

While recognising the validity of the qualitative dependences of hydrogen sorption by carbon nanomaterials doped with alkali metals,[152] Yang [153] assumed that these results might have been affected by the presence of moisture in the hydrogen used. Comparative experiments on the absorption of extremely pure (99.999%) absolutely dry and moist hydrogen by the lithium-doped VGCF obtained using the above technique [152] have shown that the adsorption was 2 mass % and 12 mass % H_2, respectively. It was assumed [153] that the anomalously high hydrogen sorption (up to 20 mass %) by the VGCF doped by Li and K [152] can be due to the formation of alkali metal hydroxides and hydrates in a humid atmosphere.

The graphite nanofibres obtained by pyrolysis of CO in the presence of Co/La_2O_3 also absorb H_2;[154] preheating of the samples at 1173 K is necessary in order to provide a high sorption efficiency (see also Ref. 148). The samples preheated at 673 K absorbed much less H_2, whereas graphite was found to be completely inert under identical conditions.

The effect of thermal treatment of a carbon material surface on the adsorption of hydrogen is shown by the data listed in Table 2. It was found that etching followed by treatment of carbon nanostructures increased their specific surfaces and the hydrogen-sorbing capacities, which resulted in the stable absorption of 5 mass % H_2 by the samples treated with a NaOH solution.[155] The VGCF-containing carbon soot obtained by catalytic pyrolysis of ethylene on nickel at 900 K adsorbs about 2.5 mass % of hydrogen at 5–7 MPa and with repetition of the cycles 'cooling to 77 K – heating to 300 K'.[3, 6]

Table 2. Effect of pretreatment of carbon nanotubes on hydrogen adsorption at p_{H_2} = 10 MPa and T = 293 K.[155]

Conditions of NT pretreatment	H_2 (mass %)
Mechanochemical treatment (30 min), etching (65% HNO_3, 72 h)	2.67
Mechanochemical treatment (30 min), etching (65% HNO_3, boiling)	1.16
Heating with NaOH (3 mol $litre^{-1}$, 1 h), washing with H_2O, drying at 373 K (2 h), calcination at 823 K (1 h), treatment with H_2SO_4 (15%, 1.5 h), heating at 373 K (10 min), washing with H_2O, drying at 373 K	5.15

Catalytic decomposition of acetylene at 1173 K in the presence of Co/SiO_2 results in the formation of carbon nanofibres.[156, 157] The sorption capacities of such metal-free carbon fibres at 10 MPa hydrogen pressure is ~ 1 mass % H_2. Although the structure of the carbon material obtained by Klyamkin *et al.*[156, 157] is similar to that of the VGCF obtained by Chambers *et al.*,[146] their sorption capacities differ strongly (1 mass % H_2 [156] and 67 mass % H_2 [146]), despite the similar behaviour of the specimens in the stage of hydrogen desorption. According to the reported data,[158] multi-walled carbon NT absorb up to 1 mass % H_2 at 10 MPa and 298 K. The amount of adsorbed H_2 increases with an increase in pressure in the range of 10–200 MPa.

The $CO : H_2$ ratio affects the specific surface of the nanocarbon fibre obtained upon pyrolysis of CO in the presence of a Fe–Ni–Cr alloy and its sorption capacity with respect to H_2: the hydrogen uptake by the VGCF decreases with an increase in the H_2 content in the starting mixture.[159]

High-precision calorimetric methods [160] were used to study the adsorption capacity of a number of carbon materials, including VGCF obtained according to the reported technique,[161] and commercial SWNT. The materials studied were found to be poor H_2 adsorbents under the experimental conditions (H_2 adsorption at 303 K, H_2 desorption at 373 K), and their adsorption capacities did not exceed that of activated carbon, which disagrees with other reported data.[146]

Ozaki *et al.*[162] compared the adsorption of hydrogen on platinum-coated carbon fibres prepared by two methods. The first method involved the preparation of a homogeneous mixture of a polymer with a metal complex followed by high-temperature carbonisation of the specimen. High-temperature activation of this specimen in water vapour or in CO_2 resulted in the migration of the metal particles to the outer surface of the carbon carrier. The second method employed a mixture of polymers, *viz.*, one

‡ Chen *et al.*[152] relate this material, which contains layered truncated graphene cones, to carbon nanotubes. In accordance with the terminology accepted by Dresselhaus [2] and by us, it should be attributed to graphite nanofibres.

which underwent pyrolysis and one which underwent carbonisation. The addition of a metal (Pt) compound to the pyrolysable polymer made it possible to deposit the metal on the walls of the pores formed upon pyrolysis. The H_2 adsorption for the material obtained according to the second method depends on the amount of platinum added: a small amount of platinum favours H_2 spillover and higher H : Pt ratios. A decrease in the H : Pt ratio with increase in the platinum concentration is due to an increase in the metal particle sizes.[162]

It was shown that thermal treatment of carbon nanofibres prepared by pyrolysis of ethylene in the presence of a Fe—Ni—Cu alloy (Fe : Ni : Cu = 85 : 10 : 5) in argon at 1273 K resulted in a noticeable increase in the amount of the stored hydrogen (up to 6.5 mass % H_2).[163] The importance of pretreatment of a specimen before hydrogen sorption has also been noted in other studies [148, 154] where the necessity of a special thermal treatment of VGCF in order to remove the chemisorbed gases has been shown. By analogy with NT (see Refs 142, 155), it may be surmised that chemical treatment of VGCF and their subsequent high-temperature annealing increase the specific surface of a VGCF and its activity with respect to H_2 adsorption. After an appropriate treatment, VGCF and NT obtained under catalytic pyrolysis conditions (carbon source: benzene or methane; precursor of the catalytically active species: ferrocene) can adsorb up to 4.0 mass % – 5.7 mass % H_2.[164] The absorption of pure hydrogen (99.999%) by graphite fibre with a parallel-laminated structure (98% of VGCF in the mixture) starts immediately without an induction period to reach 10 mass % – 13 mass % H_2 in the first cycle (Table 3). The H_2 adsorption and desorption rates are high.[166] Upon repeated adsorption – desorption cycles, the sorption capacity of the material decreases to approximately 70% of the original value, which is thought to be due to the destruction of the graphite fibre structure. The graphite nanofibre obtained by pyrolysis of acetylene and ethylene at 873 K in the presence of Ni adsorbs up to 10 mass % H_2 following keeping for 16 h at room temperature at 12 MPa. After a decrease in pressure, almost all hydrogen is released (Fig. 7).[166]

Table 3. Effect of pretreatment of a graphite nanofibre on hydrogen adsorption at p_{H_2} = 11 MPa and T = 373 K.[165]

Mean VGCF diameter /nm	Conditions of VGCF pretreatment	H_2 (mass %)
80	evacuation, 5 h, 373 K	12.38
90	treatment with 37% HCl, washing with H_2O, evacuation, 5 h, 373 K	12.82
100	dispersion in ethanol, treatment with 37% HCl, washing with H_2O, evacuation, 5 h, 373 K	10.03
125	dispersion in ethanol, treatment with 37% HCl, washing with H_2O, evacuation, 5 h, 373 K	10.1

Note. The graphite nanofibre was obtained by pyrolysis of benzene at 1373 – 1473 K in the presence of Fe and S.

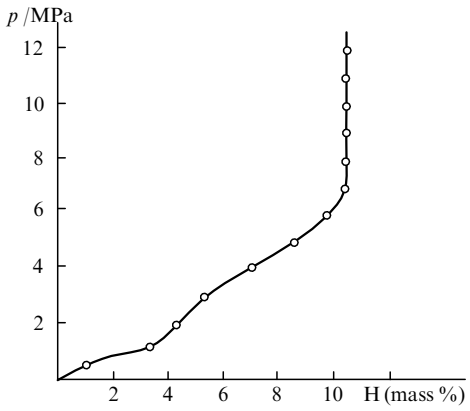


Figure 7. Hydrogen desorption isotherm at 300 K.[166]

Despite the observed discrepancies in the available experimental data (*cf.*, *e.g.*, Refs 148, 150, 158, 165), it is obvious that NT and VGCF are actually characterised by high capacities with respect to hydrogen.

3. Sorption of hydrogen by nanostructured graphite

The sorption of hydrogen on activated carbons at 133 K and p_{H_2} = 2 MPa is 0.5 g H_2 per 1 kg of C (Ref. 8) and 2 mass % at 155 K and p_{H_2} = 6.9 MPa.[150] A uniquely high, though hard to explain, hydrogen-sorbing capacity was observed for carbon of AX-21 grade with 3000 $m^2\ g^{-1}$ overall material surface and 700 – 1800 $m^2\ g^{-1}$ micropore surface; the mass and volume densities of H_2 at 77 K and 5.0 MPa were 100 g H_2 per 1 kg of the adsorbent and 32 kg H_2 per 1 m^3, respectively.[9]

The relationship between the sorption capacity and the volume of micropores has been analysed for a series of activated carbons. It has been found that a pore size optimal for the adsorption of hydrogen exists.[167]

Thermal desorption spectroscopy was used to study the sorption of hydrogen by nanoporous carbon (NPC).[168] It was shown that the maximum amount of H_2 that can be adsorbed by NPC is 15.6 at.% at 266 MPa and 773 K. Mechanochemical treatment of graphite in an extra-pure hydrogen atmosphere (99.9999%) at room temperature and starting hydrogen pressure of 1.0 MPa results in nanostructured graphite which adsorbs H_2 well.[81] After milling for 80 h, the maximum amount of adsorbed H_2 for such a sample is 7.4 mass % ($CH_{0.95}$). This value is comparable to the values of H_2 absorption reached for nanotubes and superactive carbon at temperatures below 100 K and H_2 pressures of about 5 MPa.

Enoki *et al.*[169] studied the properties of nanostructured graphite and its intercalated compounds. The composites prepared by mechanical grinding of Mg and graphite in the presence of organic additives (THF, cyclohexane, benzene) were found to be efficient hydrogen-adsorbing materials.[170, 171] The introduction of an organic additive is necessary for the composite structure to form and its hydrogen-adsorbing properties to appear.

4. Theoretical calculations of hydrogen adsorption by carbon nanomaterials

The mechanism of the uniquely high hydrogen sorption by carbon NM has not yet been clarified. Different variants have been considered: physical adsorption and chemisorption of H_2 molecules on the graphene sheet surface; the arrangement of more than one layer of H_2 molecules between the graphene planes; capillary condensation of hydrogen inside the nanotubes and in the space between the graphene sheets at anomalously high temperatures; the charge state of hydrogen in carbon nanomaterials. Therefore, the calculated maximum hydrogen capacities of NM differ strongly as well.

The Monte-Carlo method was used [172] to calculate the adsorption capacities of carbon materials with crevice-shaped and cylindrical pores with respect to gaseous H_2 at various temperatures and pressures. The calculated values of H_2 sorption were compared to the experimental results obtained for the specially prepared microporous activated carbon (AC). A linear relationship between the adsorption capacity of hydrogen and the specific surface of AC was found. The best AC samples had a specific surface of 2290 $m^2\ g^{-1}$; the corresponding maximum amount of adsorbed H_2 was 0.6 mass %. This value is in good agreement with the calculated value of 0.7 mass % H_2 for ideal slit-shaped pores with S = 2600 $m^2\ g^{-1}$ at 300 K and p_{H_2} = 6 MPa.

According to the reported data,[172] carbon materials with slit-shaped pores ($d = 0.7$ nm) are the optimum H_2 adsorbents at room temperature and $p_{H_2} = 10$ MPa. The highest calculated H_2 volume density is equal to 14 kg m^{-3} (mass content equal to 1.3 mass % H_2). According to the data of Rzepka *et al.*,[172] the sorption capacities of carbon materials with slit-shaped pores are higher than those of materials with cylindrical pores over practically the entire temperature and pressure range studied. It was noted that polymolecular (two-layer) sorption of hydrogen can be observed at 77 K in pores with $d = 1.0$ nm even at low H_2 pressures; this corresponds to the gravimetric capacity of the carbon material equal to ~ 2.0 mass % and 5.5 mass % H_2 for cylindrical and slit-shaped pores, respectively. Therefore, the observed high values of H_2 uptake by single-walled nanotubes (5 mass % – 10 mass % H_2 at room temperature)[134] cannot be explained by pure physical adsorption occurring in SWNT due to strong capillary forces.

Calculations[172] of physical H_2 adsorption at room temperature and $p_{H_2} = 11$ MPa on carbon material with slit-shaped pores with $d = 0.34$ nm corresponding to the interlayer distance in VGCF[146] imply that hydrogen cannot be adsorbed by this material. Since under these conditions the gravimetric capacity of a microporous carbon material with $d = 0.7$ nm is as low as 1.3%, the increase in d observed for VGCF in the course of hydrogen adsorption cannot result in adsorption equal to 11% – 67% reported in Ref. 146. Using the model of VGCF structure with sorbed hydrogen shown in Fig. 8 for the calculation of H_2 adsorption, it has been shown[173] that the distance of 0.34 nm between the graphene layers is insufficient for the incorporation of hydrogen molecules. Moreover, a graphite nanofibre with $d = 0.9$ nm can adsorb as low as 0.46 mass % – 1.6 mass % H_2 at 298 K and $p_{H_2} = 5 – 11.2$ MPa.

Analysis of H_2 adsorption on a graphite surface taking into account the real sorption conditions and the geometric parameters of the hydrogen molecule and the graphite layer gives the value of ~ 2.8 mass % H_2 for one H_2 layer adsorbed on a separate graphene sheet.[2] In real systems, the intermolecular forces, the interaction of the H_2 molecules with the material surface and the presence of surface defects can result in the formation of additional sites for H_2 adsorption. Considering the possible formation of the second hydrogen layer, the value of H_2 sorption on the carbon surface was assessed to be ~ 4.1 mass %.

Doping of graphite with K, Rb and Cs increases slightly its sorption capacity with respect to H_2; the H_2 content due to chemisorption corresponds to the $C_8KH_{2/3}$ composition, and the H_2 content due to physical adsorption corresponds to the $C_{24}KH_2$ composition. However, the hydrogen content is small in both cases (see Ref. 2 and the references therein). On the other hand, for VGCF doped by a metal, high H_2 absorption was obtained even at a low metal : carbon ratio (1 : 15), apparently because of partial reduction of carbon in the graphite layer due to the catalytic effect of alkali metals.[152] However, other researchers are skeptical about the high values of H_2 adsorption obtained[152] (see, for example, Refs 153 and 174), despite the elegant hypothesis put forward by Chen *et al.*[152] for the explanation of the absorption of hydrogen by nanomaterials doped by alkali metals.

Two geometrical models have been suggested for hydrogen sorption by carbon NT bundles.[2] In the first one, hydrogen is considered as a liquid capable of filling the free space unoccupied by the carbon atoms of the nanotube. The use of density values of 0.071 and 2.26 g cm^{-3} for liquid hydrogen and carbon atoms, respectively, results in the H_2 adsorption equal to 2.3 mass %. According to the second model which accounts for the adsorption of hydrogen molecules with a gas kinetics diameter of 0.289 nm both inside the SWNT and in the inter-tube space of SWNT bundles (Fig. 9), the overall H_2 adsorption for a (10,10)NT bundle[§] (the NT diameter being 1.38 nm) was found to be 4.0 mass % H_2. Of these, 3.3 mass % H_2 corresponds to the adsorption inside the tubes and 0.7 mass % H_2, to adsorption between the NT in the bundle. Under high-pressure conditions, the compressibility of hydrogen and intermolecular interaction might result in a denser packing of the hydrogen molecules and hence in an increase in its adsorption on carbon NT. In order to confirm this assumption, a detailed calculation has been carried out[175] which has shown that the density of hydrogen in this case can be, in fact, higher than follows from purely geometrical considerations.

Computer simulation of hydrogen adsorption by SWNT and a carbon material with idealised slit-shaped pores has also been carried out.[151] The hydrogen – hydrogen and hydrogen – carbon interactions were simulated using the Silvera – Goldman and Crowell – Brown potentials, respectively; quantum effects were also taken into account. Adsorption of hydrogen inside the NT, between the tubes in the bundles and on the outer SWNT surface was assumed in the calculations. The computer simulation of hydrogen absorption by SWNT and activated coal is in favour of SWNT but does not confirm the high values of hydrogen adsorption for SWNT and VGCF found experimentally.[134, 146]

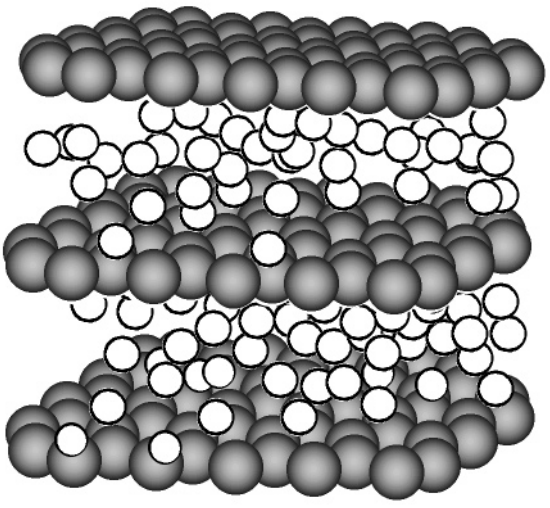


Figure 8. Cell model for the calculation of hydrogen adsorption by a platelet-type graphite nanofibre (pore diameter 0.9 nm). The dark and light circles indicate the carbon atoms and hydrogen molecules, respectively.[173]

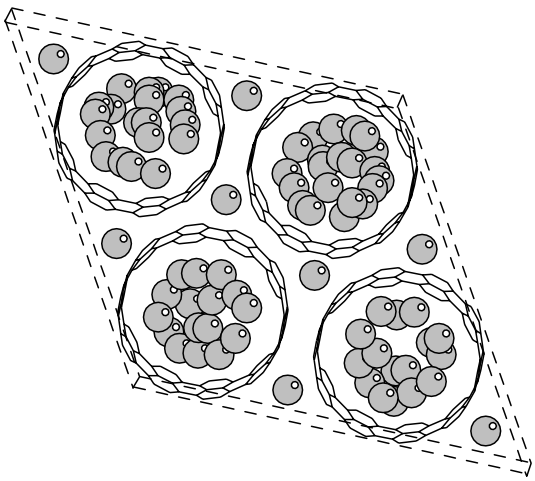


Figure 9. A typical arrangement of H_2 molecules adsorbed on triangularily packed carbon nanotubes.[2]

§ The numbers in parentheses indicate the indices used for the description of the nanotube structures; they are related directly to the NT diameter and the chiral angle.

Calculations of H_2 adsorption in SWNT bundles show [151] that the dense packing of SWNT results in lower gravimetric and volume densities of hydrogen even at sufficiently high adsorption potentials. Low adsorption can result from the surface inaccessibility in dense SWNT bundles.

The results of calculations using the Monte-Carlo method carried out for bundles of parallel SWNT demonstrate a strong dependence of the gravimetric adsorption of hydrogen on the bundle diameter, *i.e.* on its specific surface.[176] At 77 K and p_{H_2} = 10 MPa, the adsorption of H_2 for isolated (10,10)NT and for bundles consisting of three and seven (10,10)NT were 9.6 mass %, 7.0 mass % and 5.5 mass %, respectively. A dependence of the gravimetric capacity of NT on the inter-tube distance in a bundle was also noted.

The increase [138] in the inter-tube distance inside the SWNT bundles observed upon their treatment with nitric acid allows one to assume that the parameter $g = a - d$ (where g is the van der Waals gap, a is the lattice spacing, d is the NT diameter) used in the calculations of H_2 adsorption can be optimised.[177] Optimisation of the packing geometry (the g parameter) for SWNT has been carried out in order to obtain the maximum hydrogen adsorption on SWNT at 298 and 77 K. With this purpose, a series of NT have been studied, *viz.*, (9,9)NT with d = 1.22 nm, (12,12)NT with d = 1.63 nm and (18,18)NT with d = 2.44 nm. It has been found that the optimum g value is a function of temperature and equals 0.6 and 0.9 nm at 298 and 77 K, respectively.

It has been shown that none of the SWNT packing geometries studied (the triangular and square ones) can provide high hydrogen adsorption at room temperature. Hydrogen adsorption capacity approximating that recommended by the International Power Agency can be obtained on carbon NT with d = 1.22 nm and g = 0.9 nm only at 77 K and $p_{H_2} > 5$ MPa.

Calculations for charged carbon NT by the Monte-Carlo method have confirmed their somewhat higher ability to adsorb H_2 in comparison with uncharged NT: the presence of a charge results in an increase in H_2 adsorption by 10% – 20% and 15% – 30% for 298 and 77 K, respectively.[178] However, the hydrogen mass and volume densities at 298 K are still too small even for charged tubes.

Calculations using the density functional theory performed in order to search the optimum conditions of hydrogen sorption by SWNT showed that there are two types of H_2 chemisorption sites on the outer and inner NT surfaces.[179] Hydrogen is sorbed in the atomic state on the outer and inner SWNT surfaces, and also in the molecular form ¶ inside the SWNT channel.[181] The emergence of a new absorption band at 4226 cm^{-1} in the Raman spectrum of NT samples after their electrochemical charging (for gaseous H_2, 4161 cm^{-1}) assigned to the absorption of molecular hydrogen was considered as proof of the presence of adsorbed hydrogen. The H_2 capacity of cylindrical channels of carbon SWNT increases linearly with the NT diameter in accordance with the expression: c_{H_2}(mass %) $\geqslant 14.3(d/d_0)$ [where 14.3 is the amount of H_2 (in mass %) adsorbed by (10,10)NT, d_0 is the diameter of (10,10)NT]. The maximum H_2 storage capacity of carbon NT is limited by the energies of intermolecular repulsion between hydrogen molecules located in the inner SWNT cavity and those between H_2 molecules and SWNT walls.

Lee *et al.*[181] calculated the sorption of hydrogen by multilayer carbon nanotubes. Hydrogen atoms were found to be preferentially adsorbed on the outer NT surface and the sorption capacities of MWNT with respect to H_2 were found to be independent of their diameters.[181] The maximum capacities of (5,5)@(10,10)MWNT and (10,10)SWNT are 7.7 mass % and 14.3 mass % H_2, respectively.[179, 181]

¶ The inelastic neutron scattering spectra of SWNT after hydrogen adsorption on them display a peak at *ca.* 14.5 meV corresponding to rotational transitions in the H_2 molecule. The presence of this peak indicates that physical adsorption of H_2 occurs under the experimental conditions; the peak intensity decreases with a temperature increase in the range of 25 – 40 K.[180]

V. Conclusion

Carbon nanomaterials attract interest as promising materials for the development of hydrogen accumulators.

Theoretically, fullerene can be hydrogenated to $C_{60}H_{60}$ without destruction of the fullerene skeleton; this corresponds to 7.7 mass % H_2 (0.92 m^3 of H_2 per 1 kg of $C_{60}H_{60}$). However, attempts at synthesis and characterisation of the hydrofullerene with this composition have failed so far. Compound $C_{60}H_{60}$ should be extremely unstable; the excessive strain of this molecule stems from the appreciable deviation of the configuration of bonds between the carbon atoms from the most stable tetrahedral configuration. According to molecular mechanics calculations, the strain in the $C_{60}H_{60}$ molecule can be decreased if at least ten hydrogen atoms in the $C_{60}H_{60}$ molecule are bound endohedrally (this is the most stable conformation for the $C_{60}H_{60}$ composition).[182]

The methods used in practice for the reduction of fullerenes give $C_{60}H_x$ compounds with 4.5 mass % – 6.0 mass % H_2. Their preparation requires high temperatures and H_2 pressures or reactive reducing agents (see, *e.g.*, Refs 12 and 13). Analysis of numerous studies on the synthesis, structures and reactivities of hydrofullerenes shows that the practical applications of fullerenes and their metal derivatives as hydrogen sorbents require that the actual sorption capacities are increased, the hydrogenation is accelerated, the dehydrogenation temperature is decreased and the hydrogenation – dehydrogenation reversibility is ensured. In addition, side reactions should be eliminated.[3] Nevertheless, $C_{60}H_x$ and $C_{70}H_x$ hydrofullerenes have already been suggested, for example, as modifying additives for the carbon anodes of reversible Li-batteries.[183]

Other carbon nanostructures, such as single-walled carbon nanotubes and vapour-grown carbon fibres, as well as their metal-doped modifications, are quite promising as hydrogen-storage media. This is evident from Table 4 which shows generalised data on the hydrogen-sorption capacities of SWNT and VGCF, which in certain cases exceed considerably the values required for mobile hydrogen-storage systems. However, the data on the amount of hydrogen accumulated by carbon NM obtained by different authors differ considerably. The reasons for the discrepancies lie in the absence of reliable methods for the preparation of pure SWNT and VGCF and the absence of generally accepted techniques for their certification, for example, with respect to purity, degree of their 'openness', nanotube diameter and interlayer distances, and the amount of metal catalysts. In addition, the

Table 4. Sorption characteristics of various carbon nanomaterials.

Material	Maximum capacity (mass %)	T /K	p_{H_2} /MPa	Ref.
SWNT	8.25	80	7.18	137
SWNT	5 – 10	90	0.04	134
SWNT	4.2	300	10 – 12	2, 139
SWNT	6.5 – 7	300	0.1	141
SWNT	1.1 – 5.2	293	10	155
SWNT	3.5	77 ↔ 300 [a]	5 – 10	3
VGCF	11 – 67	300	11	146
VGCF	0.4	298 – 773	0.1	152
VGCF	10 – 12	373	11	166
VGCF	2.5	77 ↔ 300 [a]	5 – 10	3
Li-VGCF	20	473 – 673	0.1	152
K-VGCF	14	473 – 673	0.1	152
VGCF	10	300	12	167

[a] 'Cooling to 77 K ↔ heating to 300 K' process.

hydrogen-sorbing capacity depends crucially on the pretreatment of carbon nanomaterials and the purity of hydrogen used. Therefore, the results obtained in the studies on hydrogen sorption characterise only a particular material and cannot as yet be used for comparison of the efficiencies of different types of carbon NM. The mechanism of the uniquely high hydrogen sorption by carbon nanomaterials is not clear, either. Nevertheless, the existence of high hydrogen capacities in nanocarbon materials is obvious. This allows one to hope that nanocarbon materials (provided that they are accessible) can be used in actual hydrogen-storage systems.

The experimental and theoretical materials presented in this review testify to a significant increase in the scope of research on the synthesis and hydrogen-sorbing properties of carbon nanostructures aimed both at the solution of fundamental scientific problems and at the development of mobile hydrogen-storage systems. This is also evident from presentations submitted at various conferences on carbon nanomaterials, hydrides and hydrogen power engineering.

This review was financially supported by the Russian Foundation for Basic Research (Project Nos 99-03-32647 and 00-03-32018) and the Russian Scientific and Technical Programme (Project No. 99005).

References

1. D Yu Gamburg, V P Semenov, N F Dubovkin, L N Smirnova *Vodorod. Svoistva, Poluchenie, Khranenie, Transportirovanie, Primenenie. Spravochnoe Izdanie* (Hydrogen. Properties, Preparation, Storage, Transportation, Applications. Handbook) (Eds D Yu Gamburg, N F Dubovkin) (Moscow: Khimiya, 1989)
2. M S Dresselhaus, K A Williams, P A C Eklund *MRS Bull.* **45** (1999)
3. B P Tarasov, in *Fullereny i Fullerenopodobnye Struktury v Kondensirovannykh Sredakh* (Fullerenes and Fullerene-Like Structures in Condensed Media) (Minsk: Belorussian State University, 2000) p. 113
4. B P Tarasov, S P Shilkin *Zh. Prikl. Khim.* **68** 21 (1995) [a]
5. B A Kolachev, A A Shalin, A A Il'in, in *Splavy — Nakopiteli Vodoroda* (Alloys as Hydrogen Accumulators) (Moscow: Metallurgiya, 1995) p. 384
6. B P Tarasov *Int. Sci. J. Altern. Energy Ecology* (1) 168 (2000)
7. B P Tarasov, O N Efimov *Nauka Proizvodstvu* (10) 47 (2000)
8. J Jagiello, T J Bandosz, K Putyera, J A Schwarz *J. Chem. Soc., Faraday Trans.* **91** 2929 (1995)
9. R Chahine, T K Bose *Int. J. Hydrog. Energy* **19** 161 (1994)
10. J Withers, R Loutfy, T Love *Fullerene Sci. Technol.* **5** 1 (1997)
11. M Terrones, H W Kuang, H W Kroto, D R M Walton *Top. Curr. Chem.* **199** 189 (1999)
12. A Hirsch *Chemistry of Fullerenes* Ch. 5 (Stuttgart: Georg Thieme, 1994) p. 117
13. N F Goldshleger, A P Moravsky *Usp. Khim.* **66** 353 (1997) [*Russ. Chem. Rev.* **66** 323 (1997)]
14. A Hirsch *Top. Curr. Chem.* **199** 1 (1999)
15. B P Tarasov, V N Fokin, A P Moravsky, Yu M Shul'ga *Izv. Akad. Nauk, Ser. Khim.* 679 (1997) [b]
16. B P Tarasov, V N Fokin, A P Moravsky, Yu M Shul'ga, V A Yartys' *J. Alloys Compd.* **253–254** 25 (1997)
17. B P Tarasov, V N Fokin, A P Moravsky, Yu M Shul'ga *Zh. Neorg. Khim.* **42** 920 (1997) [c]
18. B P Tarasov *Zh. Obshch. Khim.* **68** 1245 (1998) [d]
19. B P Tarasov, V N Fokin, A P Moravsky, Yu M Shul'ga, V A Yartys', D V Schur, in *Proceedings of the 12th World Hydrogen Energy Conference, Buenos Aires, Argentina, 1998* Vol. 2, p. 1221
20. A S Lobach, B P Tarasov, Yu M Shul'ga, A A Perov, A N Stepanov *Izv. Akad. Nauk, Ser. Khim.* 483 (1996) [b]
21. N F Goldshleger, B P Tarasov, Yu M Shul'ga, A A Perov, O S Roschupkina, A P Moravsky *Izv. Akad. Nauk, Ser. Khim.* 999 (1999) [b]
22. N F Goldshleger, B P Tarasov, Yu M Shul'ga, O S Roschupkina, A A Perov, A P Moravsky, in *Fullerenes. Recent Advances in the Chemistry and Physics of Fullerenes and Related Materials* Vol. 7 (Eds K M.Kadish, P V Kamat, D Guldi) (Pennington, NJ: The Electrochemical Society, 1999) p. 647
23. B P Tarasov, V N Fokin, E E Fokina, Z A Rumynskaya, L S Volkova, A P Moravsky, Yu M Shul'ga *Zh. Obshch. Khim.* **68** 1585 (1998) [d]
24. B P Tarasov, V N Fokin, A P Moravsky, Yu M Shul'ga *Izv. Akad. Nauk, Ser. Khim.* 2093 (1998) [b]
25. Yu M Shul'ga, B P Tarasov, V N Fokin, N Yu Shul'ga, V N Vasilets *Fiz. Tv. Tela* **41** 1520 (1999) [e]
26. A M Rao, P C Eklund, U D Venkateswaran, J Tucker, M A Dunkan, G M Bendele, P W Stephens, J-L Hodeau, L Marques, M Nunez-Regueiro, I O Bashkin, E G Ponyatovsky, A P Moravsky *Appl. Phys. A, Solids Surf.* **64** 231 (1997)
27. V N Bezmelnitsyn, V P Glazkov, V P Zhukov, V A Somenkov, S Sh Shilstein, in *The 4th Biennial International Workshop in Russia 'Fullerene and Atomic Clusters' (Abstracts of Reports), St. Petersburg, 1999* p. 70
28. V P Glazkov, V P Zhukov, V A Somenkov, T N Ivanova, in *The 4th Biennial International Workshop in Russia 'Fullerene and Atomic Clusters' (Abstracts of Reports), St. Petersburg, 1999* p. 71
29. T S Ugnovenok, Yu P Udalov, I B Gavrilenko *Zh. Prikl. Khim.* **72** 1728 (1999) [a]
30. T Osaki, T Tanaka, Y Tai *Phys. Chem. Chem. Phys.* **1** 2361 (1999)
31. K Shigematsu, K Abe, M Mitani, K Tanaka *Chem. Express* **8** 37 (1993)
32. M Gerst, H-D Beckhaus, C Rüchardt, E E B Campbell, R Tellgmann *Tetrahedron Lett.* **34** 7729 (1993)
33. A Drelinkiewicz, P Byszewski, A Bielanski *React. Kinet. Catal. Lett.* **59** 19 (1996)
34. R O Loutfy, E M Veksler, A P Moravsky, in *The 4th Biennial International Workshop in Russia 'Fullerene and Atomic Clusters' (Abstracts of Reports), St. Petersburg, 1999* p. 153
35. A E Shilov, G B Shul'pin *Chem. Rev.* **97** 2879 (1997)
36. S Serizawa, I Gabrielova, T Fujimoto, T Shido, M Ichikawa *J. Chem. Soc., Chem. Commun.* 799 (1994)
37. N G Connelly, W E Geiger *Chem. Rev.* **96** 877 (1996)
38. R E Haufler, J Conceicao, L P F Chibante, Y Chai, N E Byrne, S Flanagan, M M Haley, S C O' Brien, C Pan, Z Xiao, W E Billups, M A Ciufolini, R H Hauge, J L Margrave, L J Wilson, R F Curl, R E Smalley *J. Phys. Chem.* **94** 8634 (1990)
39. Yu Vasil'ev, D Wallis, M Nüchter, B Ondruschka, A Lobach, T Drewello *Chem. Commun.* 1233 (2000)
40. G E Lawson, B Ma, H R Rollins, A M Hajduk, Y-P Sun *Res. Chem. Intermed.* **23** 549 (1997)
41. U M Dzhemilev, A G Ibragimov, L O Khafizova, L M Khalilov, Yu V Tomilov, O M Nefedov, in *The 4th Biennial International Workshop in Russia 'Fullerene and Atomic Clusters' (Abstracts of Reports), St. Petersburg, 1999* p. 31
42. U M Dzhemilev, A G Ibragimov, L O Khafizova, L M Khalilov, Yu V Vasil'ev, R F Tuktarov, Yu V Tomilov, O M Nefedov *Izv. Akad. Nauk, Ser. Khim.* 572 (1999) [b]
43. M S Meier, P K Corbin, V K Vance, M Clayton, M Mollman, M Poplawska *Tetrahedron. Lett.* **35** 5789 (1994)
44. R G Bergosh, M S Meier, J A Laske Cooke, H P Spielmann, B R Weedon *J. Org. Chem.* **62** 7667 (1997)
45. M S Meier, B R Weedon, H P Spielmann *J. Am. Chem. Soc.* **118** 11682 (1996)
46. M S Meier, J A Laske Cooke, B R Weedon, H P Spielmann, in *Fullerenes. Recent Advances in the Chemistry and Physics of Fullerenes and Related Materials* Vol. 3 (Eds K M Kadish, R S Ruoff) (Pennington, NJ: The Electrochemical Society, 1996) p. 1193
47. R G Bergosh, M S Meier, H P Spielmann, G-W Wang, B R Weedon, in *Fullerenes. Recent Advances in the Chemistry and Physics of Fullerenes and Related Materials* Vol. 4 (Eds K M Kadish, R S Ruoff) (Pennington, NJ: The Electrochemical Society, 1997) p. 241
48. P J Fagan, P J Krusic, D H Evans, S A Lerke, E Johnston *J. Am. Chem. Soc.* **114** 9697 (1992)
49. C C Henderson, C M Rohlfing, K T Gillen, P A Cahill *Science* **264** 397 (1994)
50. H P Spielmann, B R Weedon, M S Meier *J. Org. Chem.* **65** 2755 (2000)
51. A D Darwish, A K Abdul-Sada, J Langley, H W Kroto, R Taylor, D R M Walton *J. Chem. Soc., Perkin Trans. 2* 2359 (1995)
52. B R Weedon, M S Meier, H P Spielmann, in *Fullerenes. Recent Advances in the Chemistry and Physics of Fullerenes and Related Materials* Vol. 6 (Eds K M Kadish, R S Ruoff) (Pennington, NJ: The Electrochemical Society, 1998) p. 1094

53. T Tanaka, K Komatsu *J. Chem. Soc., Perkin Trans. 1* 1671 (1999)
54. T Kitagawa, Y Lee, K Takeuchi *Chem. Commun.* 1529 (1999)
55. C Rüchardt, M Gerst, J Ebenhoch, H-D Beckhaus, E E B Campbell, R Tellgmann, H Schwarz, T Weiske, S Pitter *Angew. Chem., Int. Ed. Engl.* **32** 584 (1993)
56. A S Lobach, A A Perov, A I Rebrov, O S Roshchupkina, V A Tkacheva, A N Stepanov *Izv. Akad. Nauk, Ser. Khim.* 671 (1997) [b]
57. W E Billups, W Luo, A Gonzalez, D Arguello, L B Alemany, T Marriott, M Saunders, H A Jiménez-Vázquez, A Khong *Tetrahedron Lett.* **38** 171 (1997)
58. J W Argobast, C S Foote, M Kao *J. Am. Chem. Soc.* **114** 2277 (1992)
59. S Fukuzumi, T Suenobu, S Kawamura, A Ishida, S Takamuku, S Matsumoto, K Mikami, in *The 189th Electrochemical Society Meeting (Abstracts of Reports), Los Angeles, 1996* No. 566
60. A Hirsch, T Grösser, A Skiebe, A Soi *Chem. Ber.* **126** 1047 (1993)
61. C C Henderson, P A Cahill *Science* **259** 1885 (1993)
62. S Fukuzumi, T Suenobu, S Kawamura, A Ishida, K Mikami *Chem. Commun.* 291 (1997)
63. S Fukuzumi, T Suenobu, M Patz, T Hirasaka, S Itoh, M Fujitsuka, O Ito *J. Am. Chem. Soc.* **120** 8060 (1998)
64. S Fukuzumi, M Patz, T Suenobu, A Ishida, K Mikami, in *Fullerenes. Recent Advances in the Chemistry and Physics of Fullerenes and Related Materials* Vol. 4 (Eds K M Kadish, R S Ruoff) (Pennington, NJ: The Electrochemical Society, 1997) p. 45
65. N F Goldshleger, A S Astakhova, A S Lobach, G N Boiko, N N Denisov, V A Nadtochenko, O S Roshchupkina, Yu M Shul'ga *Izv. Akad. Nauk, Ser. Khim.* 2531 (1996) [b]
66. N F Goldshleger, G N Boiko, N N Denisov, V A Nadtochenko, M G Kaplunov, A V Kulikov, in *Sb. Dokl. VII Vseros. Konf. po Metalloorganicheskoi Khimii, Moskva, 1999* (Abstracts of Reports of the VIIth All-Russian Conference on Organometallic Chemistry, Moscow, 1999) Vol. 2, p. 122
67. C S Foote *Top. Curr. Chem.* **169** 347 (1994)
68. K-F Liou, C-H Cheng *Chem. Commun.* 1423 (1996)
69. A Staško, V Brezová, S Biskupič, K-P Dinse, P Schweitzer, M Baumgarten *J. Phys. Chem.* **99** 8782 (1995)
70. V Brezová, A Staško, P Rapta, G Domschke, A Bartl, L Dunsch *J. Phys. Chem.* **99** 16234 (1995)
71. A Staško, V Brezová, P Rapta, K-D Asmus, D M Guldi *Chem. Phys. Lett.* **262** 233 (1996)
72. V Brezová, A Staško, D Dvoranová, K-D Asmus, D M Guldi *Chem. Phys. Lett.* **300** 667 (1999)
73. A Staško, V Brezová, S Biskupič, A Neudeck, A Bartl, L Dunsch, in *Fullerenes. Recent Advances in the Chemistry and Physics of Fullerenes and Related Materials* Vol. 6 (Eds K M Kadish, R S Ruoff) (Pennington, NJ: The Electrochemical Society, 1998) p. 310
74. C Siedschlag, H Luftmann, C Wolff, J Mattey *Tetrahedron* **53** 3587 (1997)
75. C Siedschlag, H Luftmann, C Wolff, J Mattey *Tetrahedron* **55** 7805 (1999)
76. D Mandrus, M Kele, R L Hettich, G Guiochon, B C Sales, L A Boatner *J. Phys. Chem. B* **101** 123 (1997)
77. R Nozu, O Matsumoto *J. Electrochem. Soc.* **143** 1919 (1996)
78. K Komatsu, Y Murata, G-W Wang, T Tanaka, N Kato, K Fujiwara *Fullerene Sci. Technol.* **7** 609 (1999)
79. K Komatsu, K Fujiwara, Y Murata, T Braun *J. Chem. Soc., Perkin Trans. 1* 2963 (1999)
80. Y Murata, N Kato, K Fujiwara, K Komatsu *J. Org. Chem.* **64** 3483 (1999)
81. S Orimo, G Majer, T Fukunaga, A Züttel, L Schlapbach, H Fujii *Appl. Phys. Lett.* **75** 3093 (1999)
82. K Komatsu, G-W Wang, Y Murata, T Tanaka, K Fujiwara, K Yamamoto, M Saunders *J. Org. Chem.* **63** 9358 (1998)
83. R S Varma *Clean Prod. Process.* **1** 132 (1999)
84. L D Field, S Sternhell, H V Wilton *Tetrahedron Lett.* **39** 115 (1998)
85. R V Bensasson, T J Hill, E J Land, S Leach, D J McGarvey, T G Truscott, J Ebenhoch, M Gerst, C Rüchardt *Chem. Phys.* **215** 111 (1997)
86. Yu M Shul'ga, B P Tarasov *Pis'ma Zh. Eksp. Teor. Fiz.* **68** 239 (1998) [f]
87. A D M Darwish, R Taylor, R Loutfy, in *Proceedings of the 197th Meeting of Electrochemical Society, Toronto, 2000* No. 693
88. I O Bashkin, V E Antonov, A I Kolesnikov, E G Ponyatovsky, J Mayers, S F Parker, J Tomkinson, A P Moravsky, Yu M Shul'ga *Mol. Mater.* **13** 251 (2000)
89. I O Bashkin, V E Antonov, O V Boltalina, I V Gol'd, A F Gurov, A I Kolesnikov, E P Krinichnaya, A P Moravsky, S S Khasanov, Yu M Shul'ga, E G Ponyatovsky *Int. Sci. J. Alternative Energy Ecology* (1) 134 (2000)
90. A I Kolesnikov, V E Antonov, I O Bashkin, J C Li, A P Moravsky, E G Ponyatovsky, J Tomkinson *Physica B* **263–264** 436 (1999)
91. A I Kolesnikov, V E Antonov, I O Bashkin, G Grosse, A P Moravsky, A Yu Muzychka, E G Ponyatovsky, F E Wagner *J. Phys., Condens. Matter* **9** 2831 (1997)
92. I O Bashkin, V E Antonov, Yu A Ossipyan, E G Ponyatovsky, A P Moravsky, Yu M Shul'ga, Yu G Morozov *Mol. Mater.* **13** 263 (2000)
93. Yu M Shul'ga, A S Lobach, Yu G Morozov, V N Spektor, A A Ovchinnikov *Zh. Fiz. Khim.* **72** 115 (1998) [g]
94. B V Lebedev, T A Bukova, A S Lobach, in *The 4th Biennial International Workshop in Russia 'Fullerene and Atomic Clusters' (Abstracts of Reports), St. Petersburg, 1999* p. 184
95. B V Lebedev, T A Bykova, A S Lobach *Dokl. Akad. Nauk* **368** 629 (1999) [h]
96. A Rathna, J Chandrasekhar *Chem. Phys. Lett.* **206** 217 (1993)
97. P A Dorozhko, A S Lobach, A A Popov, V M Senyavin, V V Yushenko, M V Korobov, in *The 4th Biennial International Workshop in Russia 'Fullerene and Atomic Clusters' (Abstracts of Reports), St. Petersburg, 1999* p. 183
98. C Jin, R Hettich, R Compton, D Joyce, J Blencoe, T Burch *J. Phys. Chem.* **98** 4215 (1994)
99. M I Attalla, A M Vassallo, B N Tattam, J V Hanna *J. Phys. Chem.* **97** 6329 (1993)
100. L E Hall, D R McKenzie, M I Attalla, A M Vassallo, R L Davis, J B Dunlop, D J H Cockayne *J. Phys. Chem.* **97** 5741 (1993)
101. D L Kepert, B W Clare *Coord. Chem. Rev.* **155** 1 (1996)
102. L D Book, G E Scuseria *J. Phys. Chem.* **98** 4283 (1994)
103. B I Dunlap, D W Brenner, G W Schriver *J. Phys. Chem.* **98** 1756 (1994)
104. M Bühl, W Thiel, U Schneider *J. Am. Chem. Soc.* **117** 4623 (1995)
105. A S Lobach, Yu M Shul'ga, A I Rebrov, A A Perov, Yu G Morozov, in *Fullerenes. Recent Advances in the Chemistry and Physics of Fullerenes and Related Materials* Vol. 4 (Eds K M Kadish, R S Ruoff) (Pennington, NJ: The Electrochemical Society, 1997) p. 246
106. A V Okotrub, L G Bulusheva, I P Asanov, A S Lobach, Yu M Shulga *J. Phys. Chem. A* **103** 716 (1999)
107. A S Lobach, V V Strelets *Izv. Akad. Nauk, Ser. Khim.* 2083 (1999) [b]
108. A V Okotrub, L G Bulusheva, I P Asanov, A S Lobach, Yu M Shul'ga *Zh. Neorg. Khim.* **45** 523 (2000) [c]
109. N N Breslavskaya, P N D'yachkov *Zh. Neorg. Khim.* **45** 499 (2000) [c]
110. L E Hall, D R McKenzie, R L Davis, M I Attalla, A M Vassallo *Acta Crystallogr., Sect. B, Struct. Sci.* **54** 345 (1998)
111. W E Billups, A Gonzalez, C Gesenberg, W Luo, T Marriott, L B Alemany, M Saunders, H A Jiménez-Vázquez, A Khong *Tetrahedron Lett.* **38** 175 (1997)
112. B W Clare, D L Kepert *J. Mol. Struct. (Theochem)* **177** 466 (1999)
113. E L Brosha, J Davey, F H Garzon, S Gottesfeld *J. Mater. Res.* **14** 2138 (1999)
114. V Ya Davydov, N Sheppard, E Osava *Int. Sci. J. Alternative Energy Ecology* (1) 183 (2000)
115. M S Meier, R G Bergosh, in *Fullerenes. Recent Advances in the Chemistry and Physics of Fullerenes and Related Materials* Vol. 6 (Eds K M Kadish, R S Ruoff) (Pennington, NJ: The Electrochemical Society, 1998) p. 1103
116. S Fukuzumi, T Suenobu, T Hirasaka, R Arakawa, K M Kadish *J. Am. Chem. Soc.* **120** 9220 (1998)
117. S Fukuzumi, T Hirasaka, T Suenobu, X Gao, K M Kadish, in *The 195th Electrochemical Society Meeting (Abstracts of Reports), Seattle, USA, 1999* No. 652
118. S Fukuzumi, T Hirasaka, T Suenobu, O Ito, M Fujisuka, X Gao, K M Kadish, in *The 195th Electrochemical Society Meeting (Abstracts of Reports), Seattle, USA, 1999* No. 729
119. L I Tkachenko, A S Lobach, V V Strelets *Izv. Akad. Nauk, Ser. Khim.* 1136 (1998) [b]
120. K Choho, G van Lier, G Van de Woude, P Geerlings *J. Chem. Soc., Perkin Trans. 2* 1723 (1996)

121. M E Niyazymbetov, D E Evans, S A Lerke, P A Cahill, C C Herderson *J. Phys. Chem.* **98** 13093 (1994)
122. D E Cliffel, A J Bard *J. Phys. Chem.* **98** 8140 (1994)
123. B L Tumanskii, O G Kalina, V V Bashilov, A V Usatov, E A Shilova, Yu I Lyakhovetskii, S P Solodovnikov, N N Bubnov, Yu N Novikov, A S Lobach, V I Sokolov *Izv. Akad. Nauk, Ser. Khim.* 1119 (1999) [b]
124. G A Domrachev, S N Titova, G V Markin, S Yu Khorshev, L V Kalutskaya, E V Ivanova, B S Kaverin, A I Kirillov, V L Karnatchevich, Yu A Kurskii, A S Shavyrin, in *Mezhdunar. Konf. 'Metalloorganicheskie Soedineniya — Materialy Budushchego Tysyacheletiya' (III Razuvaevskie Chteniya) (Tez. Dokl.), N Novgorod, 2000* [International Conference 'Organometallic Compounds are Materials of the Future Millennium (IIIrd Razuvaev Lectures) (Abstracts of Reports), N Novgorod, 2000] p. 28
125. S Iijima *Nature (London)* **354** 56 (1991)
126. R A Buyanov, in *Zakoksovanie Katalizatorov* (Coking of Catalysts) (Novosibirsk: Nauka, 1983) p. 109
127. A S Fialkov *Uglerod. Mezhsloevye Soedineniya i Kompozity na Ego Osnove* (Carbon. Interstitial Compounds and Composites Based on It) (Moscow: Aspekt-Press, 1997)
128. D Tomanek, R J Enbody (Eds) *Science and Application of Nanotubes* (New York: Kluwer Academic, Plenum, 2000)
129. A L Ivanovskii *Usp. Khim.* **68** 119 (1999) [*Russ. Chem. Rev.* **68** 103 (1999)]
130. E G Rakov *Usp. Khim.* **69** 41 (2000) [*Russ. Chem. Rev.* **69** 53 (2000)]
131. J Hu, T W Odom, C M Lieber *Acc. Chem. Res.* **32** 435 (1999)
132. P M Ajayan *Chem. Rev.* **99** 1787 (1999)
133. E G Rakov *Zh. Neorg. Khim.* **44** 1827 (1999) [c]
134. A C Dillon, K M Jones, T A Bekkedahl, C H Kiang, D S Bethune, M J Heben *Nature (London)* **386** 377 (1997)
135. A G Rinzler, J Liu, H Dai, P Nikolaev, C B Huffman, F J Rodriquez-Macias, P J Boul, A H Lu, D Heymann, D T Colbert, R S Leu, J E Fischer, A M Rao, P C Eklund, R E Smalley *Appl. Phys. A, Solids Surf.* **67** 29 (1998)
136. J Liu, A G Rinzler, H J Dai, J H Hafner, R K Bradly, P J Boul, A Lu, T Iverson, K Shelimov, C B Huffman, F J Rodriquez-Macias, Y S Shon, T R Lee, D T Golbert, R E Smalley *Science* **280** 1253 (1998)
137. Y Ye, C C Ahn, C Witham, B Fultz, J Liu, A G Rinzler, D Colbert, K A Smith, R E Smalley *Appl. Phys. Lett.* **74** 2307 (1999)
138. C Bower, A Kleinhammes, Y Wu, O Zhou *Chem. Phys. Lett.* **288** 481 (1998)
139. C Liu, Y Y Fan, M Liu, H T Cong, H M Cheng, M S Dresselhaus *Science* **286** 1127 (1999)
140. Yu M Shul'ga, B P Tarasov, E P Krinichnaya, V E Muradyan, Yu G Morozov, N Yu Shul'ga, in *Fullereny i Fullerenopodobnye Struktury v Kondensirovannykh Sredakh* (Fullerenes and Fullerene-Like Structures in Condensed Media) (Minsk: Belorussian State University, 2000) p. 41
141. M J Heben, A C Dillon, T Genett, J L Alleman, K M Jones, P K Parilla, in *International Symposium on Metal–Hydrogen Systems (Abstracts of Reports), Noosa, Australia, 2000* Vol. 2, p. 2
142. A Kuznetsova, D B Mawhinney, V Naumenko, J T Yates Jr, J Liu, R E Smalley *Chem. Phys. Lett.* **321** 292 (2000)
143. C Nützenadel, A Züttel, D Chartouni, L Schlapbach *Electrochem. Solid-State Lett.* **2** 30 (1999)
144. A S Lobach, A S Astakhova, N G Spitsyna, in *Vseros. Seminar 'Nanochastitsy i Nanokhimiya' (Tez. Dokl.), Chernogolovka, 2000* [All-Russian Seminar 'Nanoparticles and Nanochemistry (Abstracts of Reports) , Chernogolovka, 2000] p. 65
145. S Pekker, J-P Salvetat, E Jakab, J-M Bonnard, L Forro, in *Proceedings of the XIIIth International Winterschool 'Electronic Properties of Novel Materials — Science and Technology of Molecular Nanostructures', Melville, NY, 1999* (Eds H Kuzmany, J Fink, M Mehring, S Roth) p. 474
146. A Chambers, C Park, R T K Baker, N M Rodriguez *J. Phys. Chem. B* **102** 4253 (1998)
147. C D Tan, P E Anderson, N M Rodriguez, in *The 195th Electrochemical Society Meeting (Abstracts of Reports), Seattle, USA, 1999* No. 541
148. C Park, P E Anderson, A Chambers, C D Tan, R Hidalgo, N M Rodriguez *J. Phys. Chem. B* **103** 10572 (1999)
149. C C Ahn, Y Ye, B V Ratnakumar, C Witham, R C Bowman Jr, B Fultz *Appl. Phys. Lett.* **73** 3378 (1998)
150. R Ströbel, L Jörissen, T Schliermann, V Trapp, W Schütz, K Bohmhammel, G Wolf, J Garche *J. Power Sources* **84** 221 (1999)
151. Q Wang, J K Johnson *J. Chem. Phys.* **110** 577 (1999)
152. P Chen, X Wu, J Lin, K L Tan *Science* **285** 91 (1999)
153. R T Yang *Carbon* **38** 623 (2000)
154. X B Wu, P Chen, J Lin, K L Tan *Int. J. Hydrogen Energy* **25** 261 (2000)
155. H W Zhu, A Chen, Z Q Mao, C L Xu, X Xiao, B Q Wei, J Liang, D H Wu *J. Mater. Sci. Lett.* **19** 1237 (2000)
156. S N Klyamkin, K Metenier, D E Sklovsky, S Bonnamy, F Beguin, in *Carbon'99. The 24th Biennial Conference on Carbon (Abstracts of Reports), Charlestone, SC, 1999* p. 628
157. S N Klyamkin, D E Sklovsky, K Metenier, S Bonnamy, F Beguin *Mol. Mater.* **13** 367 (2000)
158. S N Klyamkin, K Metenier, D E Sklovsky, S Bonnamy, F Beguin, in *Carbon'99. The 24th Biennial Conference on Carbon (Abstracts of Reports), Charlestone, SC, 1999* p. 94
159. I M Mellor, R J Mortimer, M Turpin, in *Carbon'99. The 24th Biennial Conference on Carbon (Abstracts of Reports), Charlestone, SC, 1999* p. 622
160. T D Jarvi, J Sun, L F Conopask, S Satyapal, in *The 195th Electrochemical Society Meeting (Abstracts of Reports), Seattle, USA, 1999* No. 542
161. N M Rodriguez *J. Mater. Res.* **8** 3233 (1992)
162. J Ozaki, W Ohizumi, A Oya, M J Illan-Gomez, M C Roman-Martinez, A Linares-Solano *Carbon* **38** 778 (2000)
163. D J Browning, M L Gerrard, J B Lakeman, I M Mellor, R J Mortimer, M C Turpin, in *Proceedings of the 39th Power Source Conference-2000, Sagamor, USA, 2000* p. 192
164. S M Cheng, C Liu, Y Y Fan, F Li, G Su, H T Cong, L L He, M Liu *Z. Met.kd.* **91** 306 (2000)
165. Y Y Fan, B Liao, M Liu, Y L Wei, M Q Lu, H M Cheng *Carbon* **37** 1649 (1999)
166. B K Gupta, O N Srivastava *Int. J. Hydrog. Energy* **25** 825 (2000)
167. M A de la Casa-Lillo, D Cazorla-Amorus, A Linares-Solano, P Malbrunot, D Vidal, in *Carbon'99. The 24th Biennial Conference on Carbon (Abstracts of Reports), Charlestone, SC, 1999* p. 780
168. E A Evard, I E Gabis, S K Gordeev, in *Fullereny i Fullerenopodobnye Struktury v Kondensirovannykh Sredakh* (Fullerenes and Fullerene-Like Structures in Condensed Media) (Minsk: Belorussian State University, 2000) p. 34
169. T Enoki, Y Shibayama, B L V Plasad, H Sato *Mol. Mater.* **13** 31 (2000)
170. H Imamura, Y Takesue, T Akimoto, S Tabana *J. Alloys Compd.* **293–295** 564 (1999)
171. H Imamura, Y Takesue, S Tabata, N Shigetoni, Y Sakata, S Tsuchiya *Chem. Commun.* 2277 (1999)
172. M Rzepka, P Lamp, M A de la Casa-Lillo *J. Phys. Chem. B* **102** 10894 (1998)
173. Q Wang, J K Johnson *J. Phys. Chem. B* **103** 277 (1999)
174. F E Pinkerton, B G Wicke, C H Olk, G G Tibbetts, G P Meisner, M S Meyer, J F Herbst *J. Phys. Chem. B* **104** 9460 (2000)
175. G Stan, M W Cole *Surf. Sci.* **395** 280 (1998)
176. K A Willams, P C Eklund *Chem. Phys. Lett.* **320** 352 (2000)
177. Q Wang, J K Johnson *J. Phys. Chem. B* **103** 4809 (1999)
178. V V Simonyan, P Diep, J K Johnson *J. Chem. Phys.* **111** 9778 (1999)
179. S M Lee, Y H Lee *Appl. Phys. Lett.* **76** 2877 (2000)
180. J E Fisher *Chem. Innov.* **30** 21 (2000)
181. S M Lee, K S Park, Y C Choi, Y S Park, J M Bok, D J Bae, K S Nahm, Y G Choi, S C Yu, N-g Kim, T Frauenheim, Y H Lee *Synth. Met.* **113** 209 (2000)
182. M Saunders *Science* **253** 330 (1991)
183. US P. 6 146 791 (2000)

[a] — *Russ. J. Appl. Chem. (Engl. Transl.)*
[b] — *Russ. Chem. Bull. (Engl. Transl.)*
[c] — *Russ. J. Inorg. Chem. (Engl. Transl.)*
[d] — *Russ. J. Gen. Chem. (Engl. Transl.)*
[e] — *Phys. Solid State (Engl. Transl.)*
[f] — *J. Exp. Theor. Phys. Lett. (Engl. Transl.)*
[g] — *Russ. J. Phys. Chem. (Engl. Transl.)*
[h] — *Dokl. Chem. Technol.*, *Dokl. Chem. (Engl. Transl.)*